HOKKAIDO UNIVERSITY

Title	Studies on therapeutics of prion diseases : Establishment of novel screening method for anti-prion compounds and cell therapy model
Author(s)	単, 智夫
Degree Grantor	北海道大学
Degree Name	博士(獣医学)
Dissertation Number	甲第12617号
Issue Date	2017-03-23
DOI	https://doi.org/10.14943/doctoral.k12617
Doc URL	https://hdl.handle.net/2115/67297
Type	doctoral thesis
File Information	Zhifu_Shan.pdf

Hokkaido University Collection of Scholarly and Academic Papers : HUSCAP

Studies on the therapeutics of prion diseases
—Establishment of novel screening method for anti-prion compounds and cell therapy model—

(プリオン病の治療法に関する研究　—抗プリオン薬新規スクリーニング法と細胞治療モデルの確立)

Zhifu SHAN

CONTENTS

CONTENTS ..... **i**

ABBREVIATIONS ..... **iii**

PREFACE **1**

[Chapter I] Establishment of a simple cell-based ELISA for the direct detection of abnormal isoform of prion protein from prion-infected cells without cell lysis and proteinase K treatment

INTRODUCTION **8**

MATERIALS AND METHODS **9**

RESULTS **12**

MAb 132 discriminates prion-infected cells from uninfected cells in a cell-based ELISA 12

Performance of cell-based ELISA using mAb 132 13

Utility of cell-based ELISA in combination with cytotoxicity assay 16

Detection of PrP^{Sc}-sen and PrP^{Sc}-res by mAb 132 22

DISCUSSION **24**

BRIEF SUMMARY **29**

[Chapter II] Therapeutic effect of an autologous compact bone derived mesenchymal stem cell transplantation on prion disease

INTRODUCTION **31**

MATERIALS & METHODS **32**

RESULTS **38**

Expression of cell surface markers on CB-MSCs 38

Migration of CB-MSCs to brain extract 38

Effect of CB-MSCs on survival of prion-infected mice 40

Effect of CB-MSCs on PrP^{Sc} accumulation and neuropathology 43

DISCUSSION **48**

BRIEF SUMMARY **53**

CONCLUSION **53**

ACKNOWLEDGEMENTS **57**

REFERENCES **58**

ABBREVIATIONS

aa	Amino acid(s)
AD	Alzheimer's disease
BDNF	Brain-derived neurotrophic factor
BM-MSCs	Bone marrow-derived mesenchymal stem cells
BSE	Bovine spongiform encephalopathy
CB-MSC	Compact bone-derived mesenchymal stem cells
CDI	Conformation-dependent immunoassay
CJD	Creutzfeld-Jakob disease
CNS	Central nervous system
CV	Coefficient of variation
CWD	Chronic wasting disease
DAPI	4',6-diamidino-2-phenylindole
DMEM	Dulbecco's modified eagle medium
DW	Deionized water
dpi	Days post inoculation
ELISA	Enzyme-linked immunosorbent assay
FBS	Fetal bovine serum
FDA	Food and Drug Administration
FFI	Fatal familial insomnia
FI	Fluorescence intensities
GFAP	Glial fibrillary acidic protein
GdnSCN	Guanidine thiocyanate

GPI	Glycosylphosphatidylinositol
GSS	Gerstmann-Straussler-Scheinker
Iba-1	Ionized calcium binding adaptor molecule 1
IFA	Immunofluorescence assay
HBSS	Hanks' balanced salt solution
HE	Hematoxylin-eosin
HGF	Hepatocyte growth factor
hMSC	Human mesenchymal stem cell
HRP	Horseradish peroxidase
mAb	Monoclonal antibody
MSC	Mesenchymal stem cell
N2a	Neuro2a
NGF	Nerve growth factor
PBS	Phosphate buffered saline
PBST	PBS containing 0.1% Tween 20
PFA	Paraformaldehyde
PK	Proteinase K
PPS	Pentosan polysulfate
PrP^{C}	Cellular isoform of prion protein
PrP^{Sc}	Abnormal isoform of prion protein
PrP^{Sc}-res	PK-resistant PrP^{Sc}
PrP^{Sc}-sen	PK-sensitive PrP^{Sc}
RT	Room temperature

RT-PCR	Reverse transcription polymerase chain reaction
PVDF	Polyvinylidene difluoride
S/B	Signal-to-background ratio
ScGT1-7-22L	GT1-7 mouse immortalized hypothalamic neurons infected with the 22L strain
ScN2a-3-22L	N2a-3 cells persistently infected with the 22L prion strain
ScN2a-3-Ch	N2a-3 cells persistently infected with the Chandler prion strain
SDS-PAGE	Sodium dodecyl sulfate-polyacrylamide gel electrophoresis
S/N	Signal-to-noise ratio
TSE	Transmissible spongiform encephalopathies
VEGF	Vascular endothelial growth factor
WST	2-(4-iodophenyl)-3-(4-nitrophenyl)-5-(2,4-disulfophenyl)-2H-tetrazolium, monosodium salt

PREFACE

Prion diseases or Transmissible spongiform encephalopathies (TSE) are fatal neurodegenerative diseases including scrapie in sheep and goats, bovine spongiform encephalopathy (BSE), and chronic wasting disease (CWD) in cervid and Cretuzfeldt-Jakob disease (CJD), Gerstmann-Straüssler-Scheinker syndrome (GSS) and fatal familial insomnia (FFI) in human (Prusiner, 1994; 1998). The characteristics of prion diseases are the vacuolation of neurons and neuropil, astrocytosis and microglial activation and the accumulation of disease-specific prion protein (PrP^{Sc}), the pathological isoform of the cellular prion protein (PrP^{C}) in the central nervous system (CNS). PrP^{C} is encoded by the host gene *Prnp* and is a glycosylphosphatidylinositol (GPI) - anchoring protein that is expressed on the cell surface (Stahl *et al.*, 1987). Amino acid sequences of PrP are conserved from mammals to birds (Wopfner *et al.*, 1999).

Deletion of *Prnp* gene neither changes normal life expectancy of mouse nor shows obvious developmental defects (Bueler *et al.*, 1992). However, some defects were reported: PrP deficient mice show subtle changes in circadian rhythms (Tobler *et al.*, 1996) and impaired long-term potentiation (Collinge *et al.*, 1994). PrP^{C} is also reported to modulate neuronal excitability by reducing of afterhyperpolarization potential in hippocampal CA1 cells (Mallucci *et al.*, 2002). Recently, it is reported that PrP^{C} is essential for myelin maintenance and is involved in myelin homeostasis by interacting G-protein coupled receptor Adgrg6 (Bremer *et al.*, 2010; Kuffer *et al.*, 2016; Radovanovic *et al.*, 2005). Biochemical and cell biological studies suggested that PrP^{C} acts as a copper ion transporter (Brown *et al.*,

1997), has anti-apoptotic properties (Zanata *et al.*, 2002), and is involved in defense against oxidative stress (Klamt *et al.*, 2001). Although the physiological function of PrP^{C} is not clarified completely, it is well-known that PrP^{C} plays a key role in prion propagation and prion-induced neurodegeneration. PrP deficient mice are completely resistant to the disease (Büeler *et al.*, 1993). The expression of PrP^{C} is necessarily for the neurodegeneration and PrP^{Sc} is not a solo cause of the disease (Brandner *et al.*, 1996; Mallucci *et al.*, 2003). Moreover, the transgenic mice expressing PrP^{C} lacking GPI anchor show minimal symptoms of prion disease even though amyloid plaques type of PrP^{Sc} is heavily accumulated (Chesebro *et al.*, 2005). The knockdown of PrP^{C} expression using RNAi in mice after intracerebral inoculation of prions prevents early neuronal dysfunction and prolongs the survival of mice despite the accumulation of extra-neuronal PrP^{Sc} (White *et al.*, 2008). These findings suggest that neuropathogenesis in prion diseases is associated with the process of the conversion of PrP^{C} expressed on the cell surface to PrP^{Sc}.

PrP^{Sc} is the only known proteinaceous component of prions, the causative agent of prion diseases, and infectivity of prions is thought to be associated with PrP^{Sc} oligomers (Silveira *et al.*, 2005; Wang *et al.*, 2010). Therefore, generation of PrP^{Sc} is a key aspect of prion propagation. PrP^{Sc} is a β-sheet rich structural isomer of α-helix rich, host encoded protein, PrP^{C}. PrP^{Sc} is believed to be generated from PrP^{C} by a post-translational modification including conformational transformation. Direct interaction between PrP^{C} and the pre-existing PrP^{Sc} precedes the transformation of PrP^{C} into newly generated PrP^{Sc}. Earlier cell biological studies suggested that PrP^{Sc} is generated along with the endocytic pathway including on the cell membrane (Caughey & Raymond, 1991; Taraboulos *et al.*, 1992). However, recent progress in cell biological studies within a decade indicated the involvement of endocytic

recycling compartments and endocytic recycling pathway in PrP^{Sc} formation in cells (Marijanovic *et al.*, 2009; Yamasaki *et al.*, 2014; Yamasaki *et al.*, 2012) or PrP^{Sc} formation on the cell membrane (Goold *et al.*, 2011; Rouvinski *et al.*, 2014; Tanaka *et al.*, 2016).

Considering the mechanism of PrP^{Sc} formation and neuropathogenesis of prion diseases, there are two targets for the treatment; one is PrP-specific treatment that results in the inhibition of PrP^{Sc} formation or reduction of PrP^{Sc} level, and the other is PrP-non-specific treatment that focuses on protection of neurons from detrimental factors and/or regeneration of degenerated neural and neuronal tissues. Regarding PrP-specific treatment, inhibition of the direct binding of PrP^{C} to PrP^{Sc} and reduction of PrP^{C} expression or alteration of PrP^{C} metabolism result in the inhibition of PrP^{Sc} formation. Interference of conformational conversion of PrP^{C} to PrP^{Sc}, *e.g.*, stabilization of PrP^{C}, also results in the inhibition of PrP^{Sc} formation. Furthermore, reduction of PrP^{Sc} level by accelerating PrP^{Sc} degradation in cells is also possible target for the treatment. On the other hand, regenerative medicine is a desired candidate for PrP-non-specific treatment. Embryonic stem cells and neural stem cells are possible tools for regeneration of degenerated neurons in experimental models (Relano-Giné*s et al.*, 2011); however, there is difficulty in using these cells for clinical application because of the ethical reason. In considering autologous stem cell transplantation, induced pluripotent stem cells (iPS) that can be differentiated into multiple cell types including neurons (Chambers *et al.*, 2009; Dimos *et al.*, 2008) will be one of the choice. Mesenchymal stem cells (MSCs), which exist in tissues of mesodermal origin and can be isolated easily, are other sources of regenerative medicine with autologous cell transplantation.

Screening of chemical libraries is one of the ways to identify therapeutic compounds for prion diseases. Cells persistently infected with prions provide a good platform for analyzing

the cell biology underlying prion propagation and for screening compound libraries to identify inhibitors of PrP^{Sc} formation (Caughey & Raymond, 1991; Goold *et al.*, 2011; Marijanovic *et al.*, 2009; Taraboulos *et al.*, 1992; Veith *et al.*, 2009; Yamasaki *et al.*, 2014). For example, Kocisko *et al.* (Kocisko *et al.*, 2003) screened 2,000 Food and Drug Administration (FDA)-approved drugs using prion-infected cells and obtained 17 potent inhibitors. Ghaemmaghami et al. (Ghaemmaghami *et al.*, 2010) screened more than 10,000 compounds and identified four lead chemical scaffolds for PrP^{Sc} formation inhibitors on the basis of structure-activity relationships among 121 compounds that inhibit PrP^{Sc} formation in cells.

As the deletion of PrP gene prevented clinical onset of the disease (Büeler *et al.*, 1993) and the reduction of the PrP^{C} level by small interference RNA prolonged the survival of prion-infected mice (White *et al.*, 2008), reduction of the PrP^{C} level is also a target for the inhibition of PrP^{Sc} formation. Karapetyan *et al.* (Karapetyan *et al.*, 2013) screened 1,280 drugs approved for use in human from the US Drug Collection for their ability to decrease PrP^{C} expression in cells, and they identified Astemizole as a candidate for the treatment and prophylaxis of prion diseases. Silber *et al.* also screened large chemical libraries to find compounds that lower PrP^{C} expression in T98G human glioblastoma and IMR 32 human neuroblastoma cells using a cell-based ELISA (Silber *et al.*, 2014). Alternatively, stabilization of PrP^{C}, which inhibits the conformational transition of PrP^{C} into PrP^{Sc}, is also a target for the inhibition of PrP^{Sc} formation. *In silico* screening of compounds that are capable of binding to PrP^{C} using docking simulation has identified a new class of compounds that inhibit PrP^{Sc} formation in prion-infected cells (Ferreira *et al.*, 2014; Hosokawa-Muto *et al.*, 2009; Kuwata *et al.*, 2007).

From another side, the strategy of cell therapies with stem cells has opened a new

approach for treatment of degenerative diseases because of the potential applications in regenerative medicine. The mesenchymal stem cells (MSCs) are pluripotent cells that can be isolated from adult tissues of mesodermal origin, such as bone marrow, adipose tissue, compact bones, and umbilical cord blood (Nombela-Arrieta *et al.*, 2011). MSCs can be differentiated into various cell types, not only into mesenchymal lineage (osteocytes, chondrocytes, adipocytes, skeletal muscle cells), but also ectodermal (neuronal cells, Schwann cells) and endodermal (hepatocytes, insulin-producing pancreatic cells) lineages (Kuroda *et al.*, 2011; Snykers *et al.*, 2009). In considering the use of stem cells in cell therapy, MSCs have some advantages, such as the minimal ethical problem, extensive sources and safety (Qayyum *et al.*, 2012; Qi *et al.*, 2012).

MSCs have been reported to have beneficial effects as cell therapy in animal models of stroke (Azizi *et al.*, 1998; Chen *et al.*, 2001; Li *et al.*, 2005), spinal cord injury (Hofstetter *et al.*, 2002; Urdzikova *et al.*, 2006), brain tumor (Nakamura *et al.*, 2004), and neurodegenerative diseases such as Alzheimer's disease (AD) (Kim *et al.*, 2012; Lee *et al.*, 2010), Parkinson's Disease (Blandini *et al.*, 2010; Chao *et al.*, 2009; Hellmann *et al.*, 2006; Park *et al.*, 2012), and amyotrophic lateral sclerosis (Boucherie *et al.*, 2009; Vercelli *et al.*, 2008; Zhou *et al.*, 2013). In clinical trials of MSCs transplantation for neurological disorders also showed tendency of functional recovery or partial improvement in patients of stroke (Friedrich *et al.*, 2012; Honmou *et al.*, 2011), spinal cord injury (Yoon *et al.*, 2007), and multiple sclerosis (Karussis *et al.*, 2010). In neurodegenerative and neurological disorders, MSCs transplanted through intracerebral or intravenous route migrate to the brain lesions and ameliorate functional deficits or exhibit neuroprotective potential possibly through immunomodulation and anti-inflammatory effects by producing cytokines and chemokines or

modulating microglial activation (Lee *et al.*, 2010; Ohtaki *et al.*, 2008), neuroprotection by producing neurotrophic factors such as brain-derived neurotrophic factor (BDNF) and hepatocyte growth factor (HGF) (Bai *et al.*, 2012; Chopp & Li, 2002), neuronal differentiation or stimulation of differentiation of endogenous neural stem cells (Croft & Przyborski, 2009; Munoz *et al.*, 2005), or neurovascularization by producing vascular endothelial growth factor (VEGF) (Toyama *et al.*, 2009), or decreasing oxidative stress (Calio *et al.*, 2014). These facts demonstrate that MSCs are promising tool of cell therapy for neurodegenerative disorders.

In order to contribute to the establishment of treatment for prion diseases, in the Chapter I, I describe a novel cell-based enzyme-linked immunosorbent assay (ELISA) for the screening of anti-prion compounds, in which PrP^{Sc} can be directly detected from prion-infected cells without proteinase K (PK) treatment. In the Chapter II, I describe the effect of autologous transplantation of MSCs on the survival of mice infected with prions as a model for cell therapy of prion diseases.

Chapter I

Establishment of a simple cell-based ELISA for the direct detection of abnormal isoform of prion protein from prion-infected cells without cell lysis and proteinase K treatment

INTRODUCTION

One technical limitation in using prion-infected cells for screening anti-prion compounds is the requirement for PK treatment to remove PrP^{C} from the cell lysates. It is well known that PrP^{Sc} comprises PK-sensitive PrP^{Sc} (PrP^{Sc}-sen) and PK-resistant PrP^{Sc} (PrP^{Sc}-res) (Pastrana *et al.*, 2006; Tzaban *et al.*, 2002) and that PrP^{Sc}-sen is reported to possess higher infectivity and conversion activity than PrP^{Sc}-res (Silveira *et al.*, 2005). PK treatment is expected to digest PrP^{Sc}-sen; so when PK-treatment is used, the effect of compounds on PrP^{Sc} formation may be overlooked. Thus it is meaningful to establish a novel screening methods for anti-PrP compounds in which both PrP^{Sc}-sen and PrP^{Sc}-res can be detected without PK treatment.

Recently, my laboratory reported that the anti-PrP monoclonal antibody (mAb) 132, which recognizes amino acids 119–127 of PrP, is useful for PrP^{Sc} detection in cells and frozen tissue sections of animals infected with prions (Sakai *et al.*, 2013; Yamasaki *et al.*, 2012). Although fixation and treatment of cells or tissue sections with guanidinium salts are prerequisite, this method does not require PK treatment for the discrimination of PrP^{Sc} from PrP^{C}. To take advantage of this, I established a cell-based ELISA in which PrP^{Sc} is directly detected in cells without preparation of cell lysates and PK treatment. The cell-based ELISA established in this study provides a simple and practical method for the primary screening of anti-prion compounds.

MATERIALS AND METHODS

Antibodies and regents

The anti-PrP mAbs 132, 31C6, and 44B1, which recognize amino acids 119–127, 143–149, and discontinuous epitopes of mouse PrP, respectively, were used (Kim *et al.*, 2004b). Anti-feline parvovirus subgroup mAb P2-284 was used as a negative control antibody. (Horiuchi *et al.*, 1997) ECL™ anti-mouse IgG, horseradish peroxidase (HRP)-linked $F(ab')_2$ fragment from sheep was purchased from GE Healthcare. The Alexa Fluor 488 $F(ab')_2$ fragment of goat anti-mouse IgG (H+L) was purchased from Life Technologies. Pentosan polysulfate (PPS) was purchased from Dainippon Sumitomo Pharma and U18666A was purchased from Sigma-Aldrich.

Cell culture

N2a-3 cells, a subclone of the N2a mouse neuroblastoma cell line (Uryu *et al.*, 2007) and N2a-3 cells persistently infected with the 22L prion strain (ScN2a-3-22L) (Nakamitsu *et al.*, 2010) or the Chandler prion strain (ScN2a-3-Ch) (Uryu *et al.*, 2007) were used. GT1-7 mouse immortalized hypothalamic neurons (Schatzl *et al.*, 1997) that are persistently infected with the 22L prion strain (ScGT1-7-22L) (Yamasaki *et al.*, 2012) were also used.

Cell-based ELISA

N2a-3 and ScN2a-3-22L cells were seeded into 96-well plates (Thermo Scientific) at a

density of 1×10^4 cells/100 μl/well and cultured for 24 h. Cells were then freshly fed with the medium with or without anti-prion compounds and incubated for 48 h. After the removal of medium, cells were fixed with 50 μl/well of 4% paraformaldehyde (PFA) in phosphate-buffered saline (PBS) for 10 min at room temperature (r.t.). After the removal of PFA, 100 μl of 0.1% Triton X-100 and 0.1 M glycine in PBS was added to each well to permeabilize the cell membrane and quench residual PFA. The plates were then incubated for 10 min at r.t. After the removal of glycine and Triton X-100, the cells were treated with 50 μl of 5 M guanidine thiocyanate (GdnSCN) for 10 min at r.t. Cells were then washed once with PBS and blocked with 5% skim milk in PBS for 30 min at r.t. Immunostaining was carried out using anti-PrP mAb 132 (1 μg/ml) as the primary antibody for at least 6 h at 4 °C and diluted (1:5,000) horseradish peroxidase (HRP)-conjugated anti-mouse IgG as the secondary antibody for 1 h at r.t. Finally, antigen-antibody complexes were detected with the colorimetric HRP substrate 3,3′,5,5′-tetramethylbenzidine (Sigma). After incubation for 15 min at r.t, the reaction was stopped by adding sulfuric acid to 0.25 M and optical density at 450 nm was measured using a microplate reader (Infinite M200 Pro, Tecan). In some cases, the cytotoxicity assay described below was carried out immediately before fixation of the cells.

Cytotoxicity assay (WST assay)

After removal of the medium, the cells were washed with Opti-MEM without phenol red (Gibco) and subjected to the 2-(4-iodophenyl)-3-(4-nitrophenyl)-5-(2,4-disulfophenyl)-2H tetrazolium, monosodium salt (WST) cytotoxicity assay using Cell Counting Kit 8 (CCK-8; DojinDo). CCK-8 reagent was diluted 1:100 with Opti-MEM (Thermo) and added to each

well (100 μl/well). After incubation at 37 °C for 1 h, the absorbance at 450 nm was measured using a microplate reader.

Immunoblot analysis

Sodium dodecyl sulfate-polyacrylamide gel electrophoresis (SDS-PAGE) and immunoblotting for PrP^{Sc} detection were carried out as described elsewhere. (Nakamitsu *et al.*, 2010; Uryu *et al.*, 2007)

Dot-blotting

N2a-3 and ScN2a-3-22L cells were cultured for 72 h in 6-well plates. Cells were lysed with 200 μl/well of lysis buffer [0.5% Triton X-100, 0.5% sodium deoxycholate, 150 mM NaCl, 5 mM EDTA, and 10 mM Tris-HCl (pH 7.5)] and the protein concentration of the lysate was measured using a DC protein assay kit (Bio-Rad). Cell lysates equivalent to 40 μg of total protein were transferred onto a polyvinylidene difluoride (PVDF) membrane using a dot-blotter (Bio-Rad). The PVDF membrane was treated with PK (10 μg/ml), or not, for 1 h at r.t, and then PK digestion was terminated by the addition of Pefabloc (Roche) to 1 mM for 15 min at 4℃. The membrane was then treated with 50 μg/ml DNase I for 15 min and subsequently with 3 M GdnSCN for 30 min at r.t. For the detection of PrP, the membrane was incubated with mAb 132 (1 μg/ml) in 1% skim milk-PBS containing 0.1% Tween 20 (PBST) at 4℃ overnight. After washing the membrane with PBST, HRP-conjugated anti-mouse IgG was used as the secondary antibody for 1 h at r.t. ECL Western Blotting Detection Reagents (GE Healthcare) and a LAS-3000 chemiluminescence image analyzer (Fujifilm) were used to visualize the immune-reactive proteins.

Immunofluorescence assay (IFA)

PrP^{Sc}-specific immunofluorescence staining using mAb 132 and quantitative analysis of the signals were performed as described previously (Yamasaki *et al.*, 2014b; Yamasaki *et al.*, 2012).

Calculation of coefficient of variation (CV), signal-to-background ratio (S/B), and signal-to-noise ratio (S/N)

Forty-eight wells were seeded with N2a-3 cells and another 48 wells were seeded with ScN2a-3-22L at the density of 1×10^4 cells/100 μl/well. After 72 h incubation, the PrP signals were detected as described in the section entitled "Cell-based ELISA." Twenty-well sections were assigned for staining with mAb 132 or mAb P2-284 (negative control mAb), and the remaining eight wells were assigned as blank wells. Four independent experiments were carried out to calculate CV, S/B, and S/N. The formulas were described in the footnote of Table 1.

RESULTS

MAb 132 discriminates prion-infected cells from uninfected cells in a cell-based ELISA

First I examined whether anti-PrP mAbs 31C6, 44B1, and 132 could discriminate prion-infected cells from prion-uninfected cells by direct staining of cells. Cells grown in 96-well plates were fixed with PFA and treated briefly with GdnSCN to denature PrP^{Sc}, and

subsequently subjected to immunostaining. The mAbs 31C6 and 44B1 gave higher signals from ScN2a-3-22L cells, N2a-3 cells persistently infected with the 22L prion strain, than from prion-uninfected N2a-3 cells when these cells were pretreated with GdnSCN (Fig. I-1). However, compared with the negative control mAb, these mAbs also showed positive signals from prion-uninfected N2a-3 cells, indicating that these mAbs are not suitable for the specific detection of PrP^{Sc} in prion-infected cells. In contrast, mAb 132 showed a positive reaction only when prion-infected cells were pretreated with GdnSCN. Absorbances obtained by mAb 132 staining from uninfected cells or GdnSCN-untreated prion-infected cells remained at levels comparable with the corresponding signals obtained using the negative control antibody. Thus, among the antibodies tested, only mAb 132 could distinguish prion-infected cells from uninfected cells in a cell-based ELISA.

Performance of cell-based ELISA using mAb 132

Next I examined the dynamic range of the cell-based ELISA. ScN2a-3-22L cells were two-fold serially diluted with N2a-3 cells, and a total of 10,000 cells per well were seeded in a 96-well plate. The reaction became positive when 12.5% of cells in the well were prion-infected cells, and the signal was still in the linear range when all the cells were prion-infected cells (Fig. I-2). These results indicate that the cell-based ELISA has approximately a 1 log dynamic range. Although it was expected that some uninfected cells became infected during the 72-h incubation, the spread of infection did not influence the interpretation because I obtained the linear increase of OD_{450} in parallel with the ratio of infected and uninfected cells.

To examine whether mAb 132 is applicable to other prion strains or other cells, I used

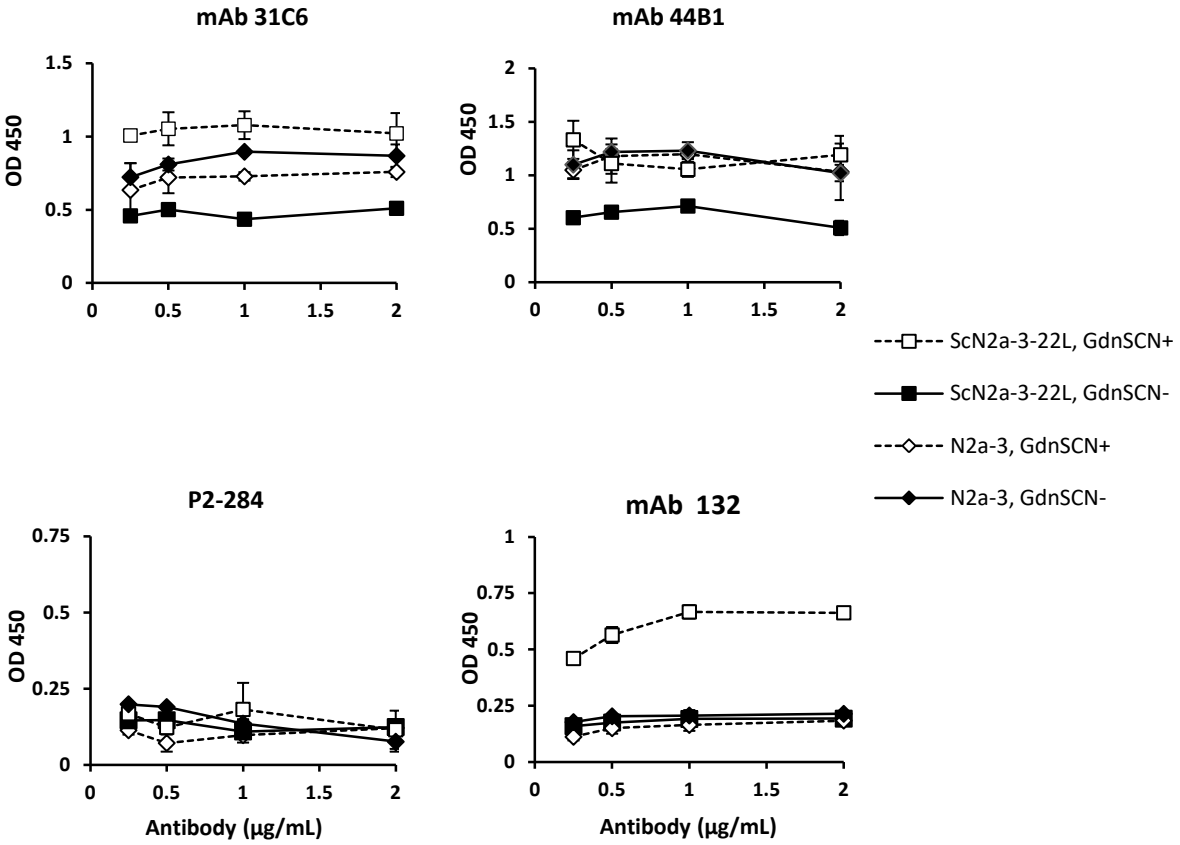

Figure I-1. MAb 132 discriminates prion-infected cells from uninfected cells in cell-based ELISA.

Prion-infected cells (ScN2a-3-22L) and uninfected cells (N2a-3) were cultured in 96-well plates for 72 h. Cells were then fixed with PFA, permeabilized with Trion X-100, and treated with (GdnSCN+) or without (GdnSCN–) 5 M GdnSCN. After blocking, the cells were subjected to immunostaining with various anti-PrP antibodies at the indicated concentrations. MAb P2-284 was used as a negative control.

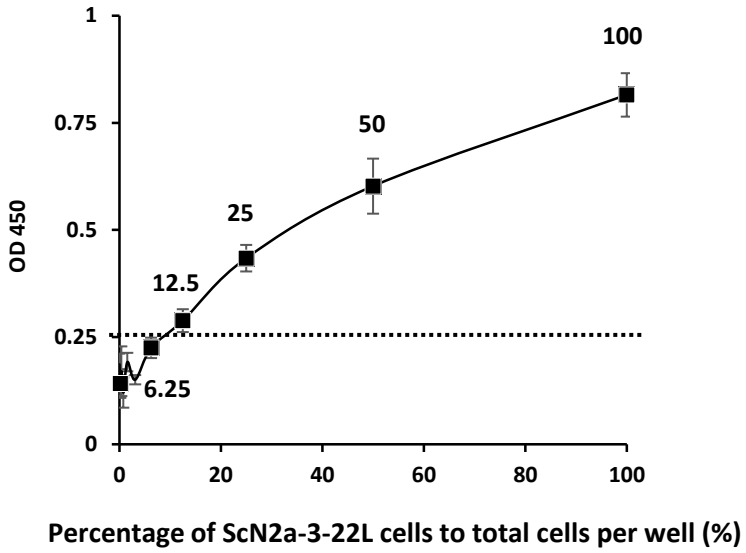

Figure I-2. Dynamic range of PrP^{Sc} detection in cell-based ELISA.
ScN2a-3-22L cell suspension (1.0×10^5 cells/ml) was two-fold serially diluted with a N2a-3 cell suspension of the same concentration. Cell suspensions (10,000 cells/100μl/well) were added to wells and incubated for 72 h. After the incubation, the cells were subjected to PrP^{Sc} detection with mAb 132. The cutoff value (dotted line) was determined as the mean plus 3 × SD of the N2a-3 signal. Numbers with plots indicate percentages of ScN2a-3-22L cells to total cells in well.

N2a-3 cells infected with the Chandler prion strain (ScN2a-3-Ch) and GT1-7 mouse immortalized hypothalamic neurons infected with the 22L prion strain (ScGT1-7-22L). The mAb 132 showed positive reaction to ScN2a-3-Ch and to ScGT1-7-22L cells (Fig. I-3). These immortalized hypothalamic neurons infected with the 22L prion strain (ScGT1-7-22L). The mAb 132 showed positive reaction to ScN2a-3-Ch and to ScGT1-7-22L cells (Fig. I-3). These results suggested that the cell-based ELISA is applicable to different prion strains and cell types.

To evaluate the performance of the cell-based ELISA, basic indices of the PrP^{Sc} detection were analyzed (Table I-1). The CV, which is the standard index for measuring variability, and is ideally <10% when measuring intra-assay variability, was approximately 10%. The S/B, which is the standard index for acceptable breadth for determining negative and positive responses, and which is ideally >2, was 2.6–3.6. The S/N, which is index for signal intensity level to background fluctuations, and which should desirably be >10, was 14.7–27.3. These indices demonstrate the reproducibility of the cell-based ELISA.

Utility of cell-based ELISA in combination with cytotoxicity assay

If the cytotoxicity of test compounds could be assessed before PrP^{Sc} detection, all the procedures of the cell-based ELISA, from the cell culture, assessment of cytotoxicity, to the immunological detection of PrP^{Sc}, could be competed with in the same plate. Thus, I examined if the WST assay affects the following PrP^{Sc} detection. Cells were treated with U18666A (Klingenstein *et al.,* 2006) or PPS (Caughey & Raymond, 1993), which are known as inhibitors for PrP^{Sc} formation, for 48 h and the WST assay was performed immediately before PrP^{Sc} detection. When ScN2a-3-22L cells were treated with U18666A, cell viability

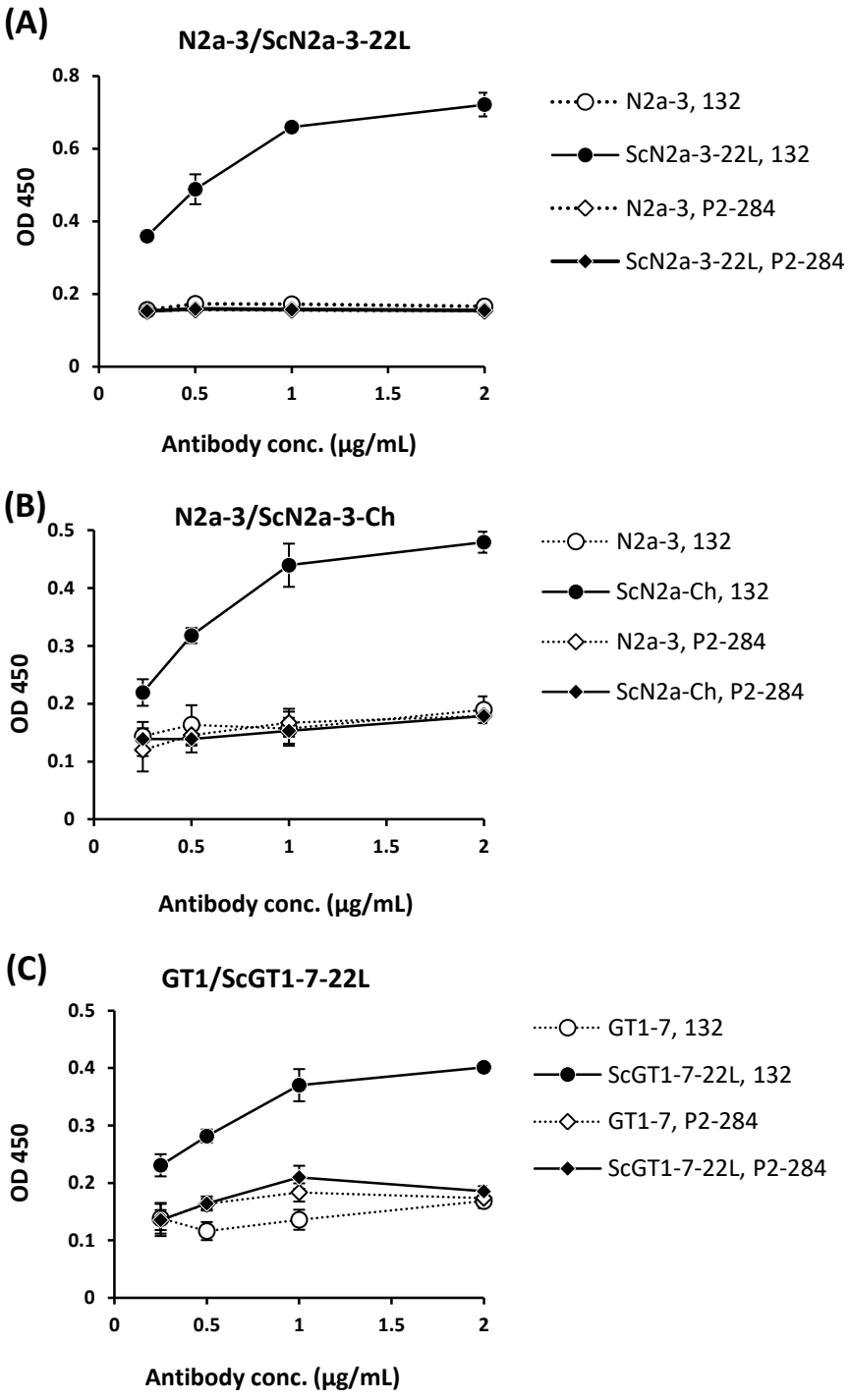

Figure I-3. Detection of PrP^{Sc} of other prion strains and from other cell types.
N2a-3 cells persistently infected with the 22L (ScN2a-3-22L), and the Chandler prion strain (ScN2a-3-Ch), and GT1-7 cells infected with the 22L prion strain (ScGT1-7-22L), were cultured in 96-well plates. After 72 h incubation, the cells were denatured by 5 M GdnSCN for 10 min and subjected to PrP^{Sc} detection with mAb 132 (open and closed circles). MAb P2-284 (open and closed diamonds) was used as a negative control mAb.

Table 1. Reliability of novel cell-based ELISA

	N2a-3	ScN2a-3-22L
OD_{450} (Average ± SD)	0.145 ± 0.026	0.635 ± 0.081
CV (%)[a]	9%–11%	7%–11%
S/B[b]	2.54–3.35	
S/N[c]	14.72–27.33	

[a]Coefficient of variation = SD/average × 100

[b]Signal-to-background ratio = $Av_{ScN2a-3-22L}/Av_{N2a-3}$

[c]Signal-to-noise ratio = $(Av_{ScN2a-3-22L} - Av_{N2a-3})/SD_{N2a-3}$

gradually decreased and obvious cytotoxicity was observed at U18666A concentrations >5 μM. PrP^{Sc} detection using mAb 132 also decreased with increasing U18666A concentration and became lower than cut off a value at U18666A concentrations >5 μM (Fig. I-4A). However, no remarkable differences in levels of PrP^{Sc} detection were observed with (ScN2a-3-22L, WST+) or without (ScN2a-3-22L, WST−) the WST assay (Fig. I-4A, see <5 μM U18666A). This result indicates the WST assay has little effect on the subsequent PrP^{Sc} detection. In contrast to U18666A, PPS treatment showed no cytotoxicity even at the highest concentration tested, while PPS drastically decreased PrP^{Sc} levels to below the cutoff value at low concentrations (Fig. I-4B). These results demonstrate that the effect of test compounds on PrP^{Sc} formation and their cytotoxicity can be assessed in the same plate. In Figure I-4B, low dose PPS treatment appeared to enhance cell viability; however those were among experimental variations and we confirmed that the low dose PPS treatment did not influence the viability of N2a-3 and ScN2a-3-22L cells (data not shown).

To confirm the accuracy of PrP^{Sc} detection after U18666A or PPS treatment in the cell-based ELISA, I analyzed PrP^{Sc} in PPS- or U18666A-treated cells by IFA (Fig. I-4C) and PrP^{Sc}-res by immunoblot analysis (Fig. I-4E). In IFA, PrP^{Sc} signals were decreased but were still detected after treatment with 5 μM U18666A and further weakened at 20 μM U18666A (Fig. I-4C). The expressions of PrP^{C} in N2a-3 and N2a-3-22L cells were confirmed by mAb 31C6 without pretreatment of cells with GdnSCN (Fig. I-4D). The result of the immunoblot analysis of U18666A-treated cells was consistent with that of the IFA (Fig. I-4E). In contrast, treatment of cells with 5 μg/ml PPS decreased PrP^{Sc} signals to levels comparable with those seen in cells treated with 20 μg/ml PPS. The gradual decrease in PrP^{Sc} levels with the increase of U18666A but drastic decrease in PrP^{Sc} levels at PPS concentrations <5 μg/ml of PPS, is

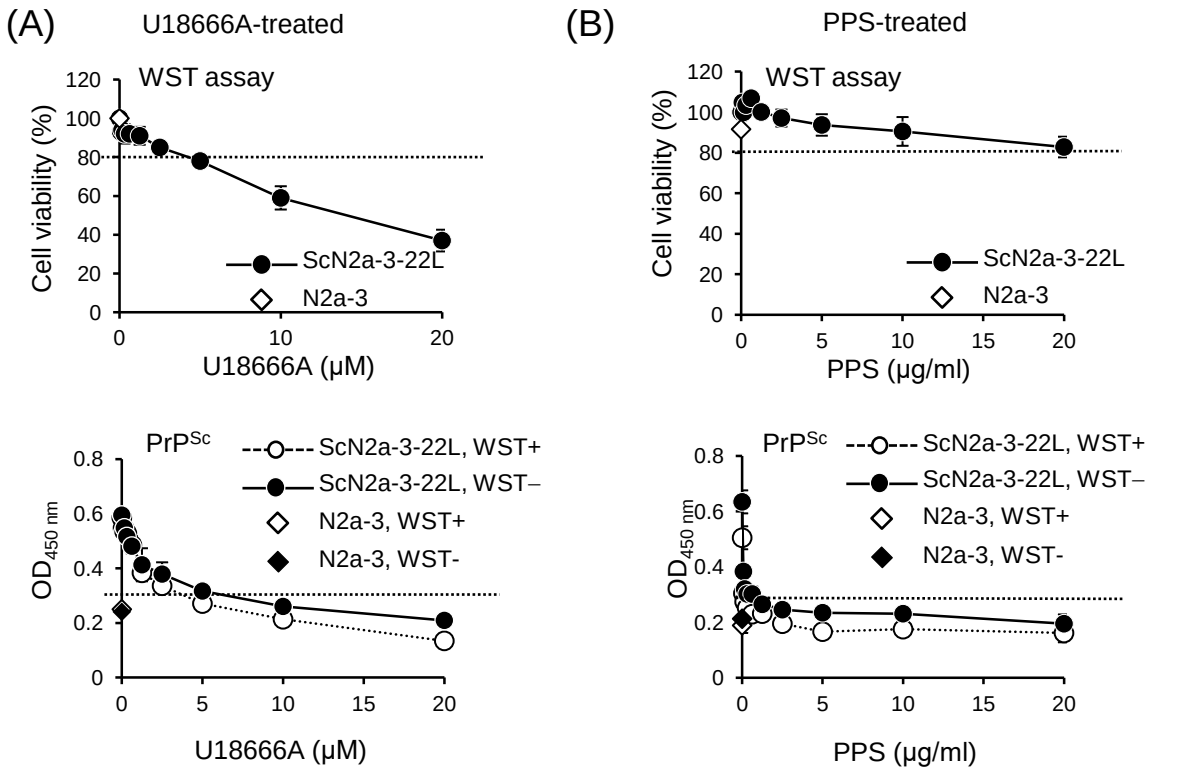
(A)
U18666A-treated
WST assay
Cell viability (%)
ScN2a-3-22L
N2a-3
U18666A (μM)
PrP^Sc
ScN2a-3-22L, WST+
ScN2a-3-22L, WST–
N2a-3, WST+
N2a-3, WST-
OD450 nm
(B)
PPS-treated
PPS (μg/ml)

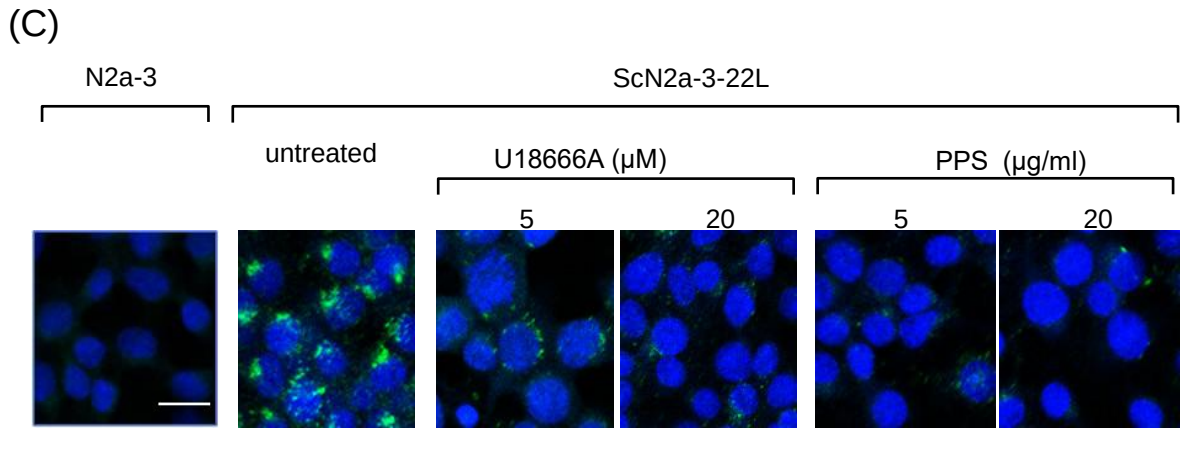
(C)
N2a-3
ScN2a-3-22L
untreated
U18666A (μM)
PPS (μg/ml)
5
20

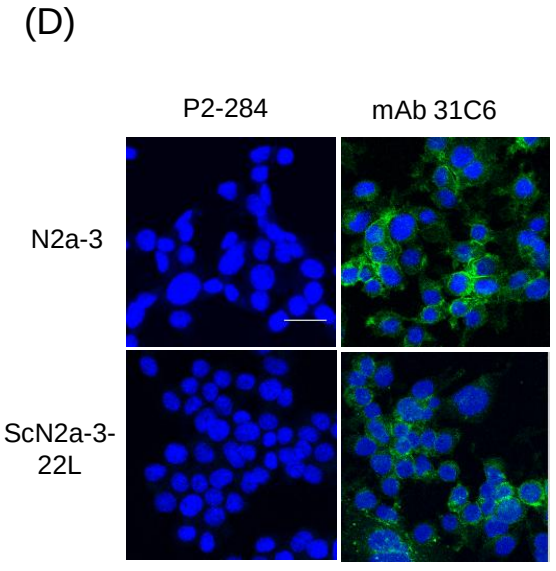
(D)
P2-284
mAb 31C6
N2a-3
ScN2a-3-22L

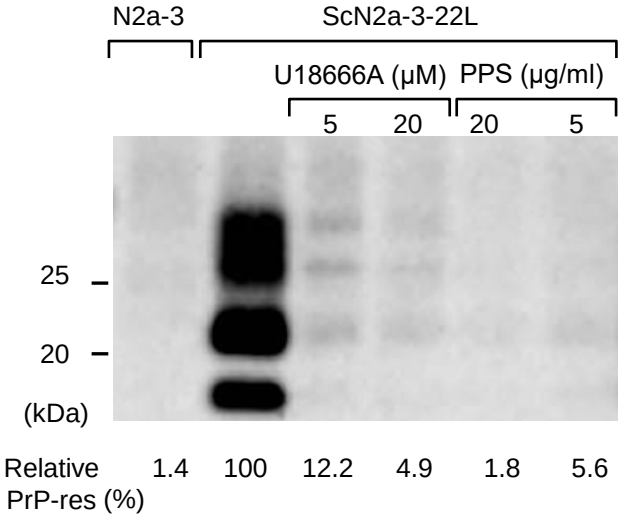
(E)
N2a-3
ScN2a-3-22L
U18666A (μM)
PPS (μg/ml)
5
20
20
5
25
20
(kDa)
Relative PrP-res (%)
1.4
100
12.2
4.9
1.8
5.6

Figure I-4. Utility of cell-based ELISA in combination with cytotoxicity assay.
(A and B) Influence of the cytotoxicity assay on subsequent PrP^{Sc} detection. ScN2a-3-22L cells were cultured in 96-well plates for 24 h and then incubated with U18666A (A) or PPS (B) for 48 h at the indicated concentrations. Immediately before fixation, cell viability was measured with the WST assay using CCK-8. After removal of the CCK-8 reagent, cells were subjected to PrP^{Sc} detection in the same plate. Regarding PrP^{Sc} detection, PrP^{Sc} signals detected after the WST assay (WST+, open diamonds and circles) or without WST assay (WST–, closed diamonds and circles) are shown. The dashed lines in WST assay indicate survival rate at 80%. The PrP^{Sc} signal detected from N2a-3 cells was used to calculate cutoff values (mean plus 3 × SD) for PrP^{Sc} detection (dashed lines). (C) IFA for PrP^{Sc} detection**.** ScN2a-3-22L cells were cultured in a chambered coverglass for 24 h and then treated or with U18666A or PPS for 48 h at the indicated concentrations. ScN2a-3-22L and N2a-3 cells untreated with these compounds were used as positive and negative controls for PrP^{Sc}, respectively. The cells were subjected to PrP^{Sc}-specific straining with mAb 132 (green), and cell nuclei were counterstained with 4', 6-diamidino-2-phenylindole (DAPI) (blue). (D) Expression of PrP^{C} in N2a-3 and ScN2a-3-cells. Cells were stained with mAb 31C6 (green) without pretreatment of GdnSCN for the detection of PrP^{C}. Nuclei were counterstained with DAPI (blue). P2-284: negative control mAb. (E) Immunoblot analysis. ScN2a-3-22L cells were cultured in 24-well plates for 24 h and subsequently treated with U18666A or PPS for 48 h at the indicated concentrations. Cells were then subjected to immunoblot analysis for the detection of PrP^{Sc}-res. N2a-3 cells untreated with these compounds were used as negative controls for PrP^{Sc}-res. PrP^{Sc}-res levels relative to untreated ScN2a-3-22L cells are shown at the bottom. Scale bars: 20 μm.

consistent with those obtained with the cell-based ELISA, demonstrating the utility of the cell-based ELISA for screening anti-prion compounds.

Detection of PrP^{Sc}-sen and PrP^{Sc}-res by mAb 132

Since the cell-based ELISA established here does not require PK treatment for PrP^{Sc} detection, it is possible that both PrP^{Sc}-res and PrP^{Sc}-sen could be detected using mAb 132, even if not all the PrP species are detected. To assess this possibility, lysates from N2a-3 and ScN2a-3-22L cells were blotted onto PVDF membranes, and after PK treatment and subsequent GdnSCN exposure (or in the reverse order), the membranes were probed with mAb 132.

No PrP was detected from the lysates of N2a-3 or ScN2a-3-22L cells lacking both PK and GdnSCN treatment (Fig I-5A, I). PrP was detected in the lysate of ScN2a-3-22L cells when the membrane was not treated with PK but treated with GdnSCN (Fig I-5A, II). These signals represent PrP^{Sc} because no PrP was detected from the lysate of N2a-3 cells under the same condition. However, the intensity of PrP^{Sc} signals decreased to approximately 40% of those seen in Fig. I-5A II when the PVDF membrane was first treated with PK and then with GdnSCN (Fig I-5A, III, and I-5B). The PrP^{Sc} signals detected under these conditions were considered to be those from PrP^{Sc}-res and the decrease in the PrP^{Sc} signal accounted for the digestion of PrP^{Sc}-sen by PK. When the PVDF membrane was treated with GdnSCN but not PK (Fig. I-5A, IV), PrP^{Sc} levels were as high as those obtained in Fig. I-5A II, suggesting that the signal accounted for the sum of PrP^{Sc}-sen and PrP^{Sc}-res. When the membrane was first treated with GdnSCN and then treated with PK, no PrP signals were obtained, since PrP^{Sc} denatured by GdnSCN was digested with PK (Fig. I-5A, V). The presence of PrP^{C} in the

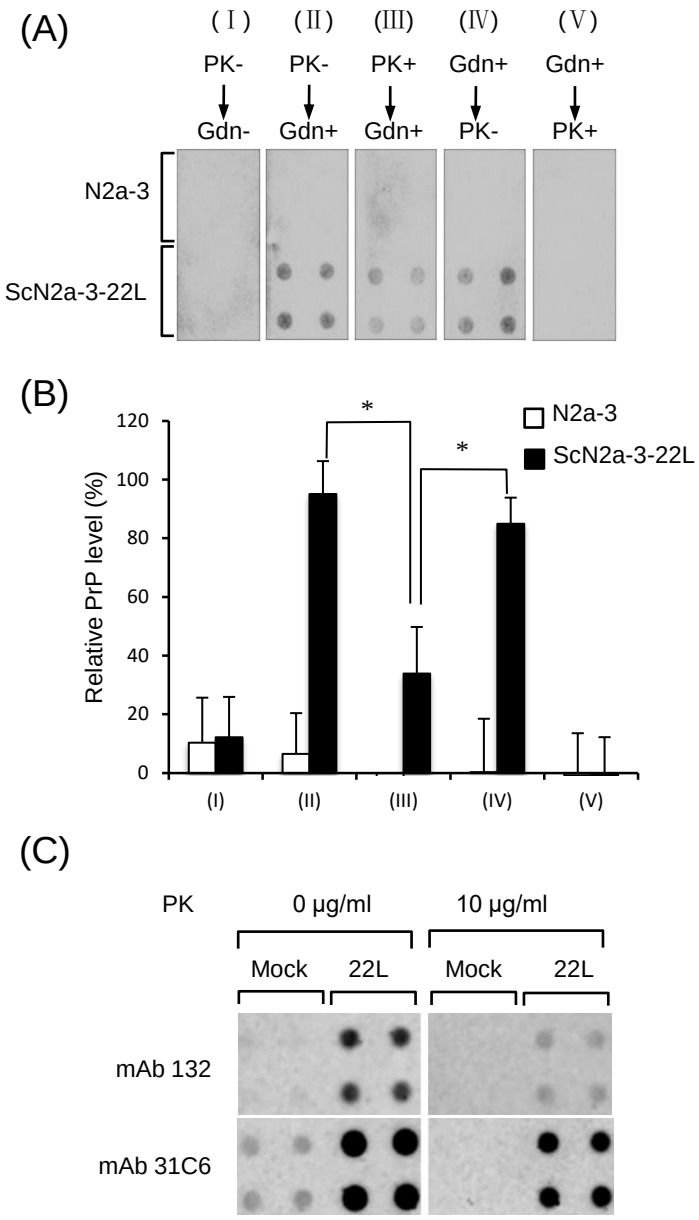

Figure I-5. Detection of PrP^{Sc}-sen and PrP^{Sc}-res by mAb 132 in a dot-blot analysis.

(A) Dot-blot analysis. Lysates from N2a-3 or ScN2a-3-22L cells were transferred onto PDVF membranes using a dot-blotter (quadruplicates). The membranes were treated with PK (10 μg/ml; PK+) (III) or not (PK–) (I and II) for 1 h at r.t. and subsequently with (Gdn+) (II and III) or without (Gdn–) 3 M GdnSCN (III) for 30 min at r.t, or in the reverse order (IV and V). Then, the membranes were stained with mAb 132, and chemiluminescence signals were detected and quantified with a LAS 3000 chemiluminescence image analyzer. The PrP levels (%) relative to the PrP level in II, detected using mAb 132, are shown in (B). *, $p < 0.05$, Student's t-test). (C) Confirmation of PrP^{C} in dot-blot analysis. Lysates from N2a-3 (Mock) or ScN2a-3-22L (22L) cells were blotted onto PDVF membranes (quadruplicates). The membranes were treated with PK (10 μg/ml) or not (0 μg/ml) for 1 h at r.t. After the termination of PK digestion, the membranes were treated with DNase I and then with 3 M GdnSCN for 30 min at r.t. as described in Materials and Methods. Finally membranes were stained with mAbs 132 and 31C6 for chemiluminescence detection.

lysate of N2a-3 was confirmed with mAb 31C6 (Fig. I-5C).

To further examine whether mAb 132 detects PrP^{Sc}-sen, ScN2a-3-22L cells were treated with low concentrations of PK and then subjected to PrP^{Sc}-specific immunostaining. The fluorescent intensities of PrP^{Sc} signals in PK-treated ScN2a-3-22L cells decreased to less than a half of those in PK-untreated ScN2a-3-22L cells, even at the lowest PK concentration tested (Fig. I-6, 0.31 μg/ml). The decrease in fluorescence intensities of PrP^{Sc} signals by PK treatment supported the idea that mAb 132 detected both PrP^{Sc}-sen and PrP^{Sc}-res.

DISCUSSION

My laboratory has reported that mAb 132, which recognizes an epitope consisting of mouse PrP aa 119–127, can specifically detect PrP^{Sc} from prion-infected cells or tissues without the removal of PrP^{C} by PK treatment (Sakai *et al.*, 2013; Yamasaki *et al.*, 2012). This feature of mAb 132 facilitated the establishment of a novel cell-based ELISA in which PrP^{Sc} levels in prion-infected cells are assessed without the removal of PrP^{C}. As anticipated, mAb 132 was the only anti-PrP mAbs tested that could distinguish prion-infected cells from uninfected cells (Fig. I-1). Signals obtained from uninfected cells and GdnSCN-untreated prion-infected cells probed with mAb 132 were comparable with signals obtained using a negative control mAb, providing a suitable S/B ratio (Table I-1). MAb 132 reacted poorly with PrP^{C} on the cell surface (Kim *et al.*, 2004a), but reacted with PrP^{Sc}, PrP^{C} and recombinant PrP in immunoblot analysis (Kim *et al.*, 2004b). Thus, mAb 132 appears to recognize a linear epitope that becomes antibody-accessible after denaturation of the PrP

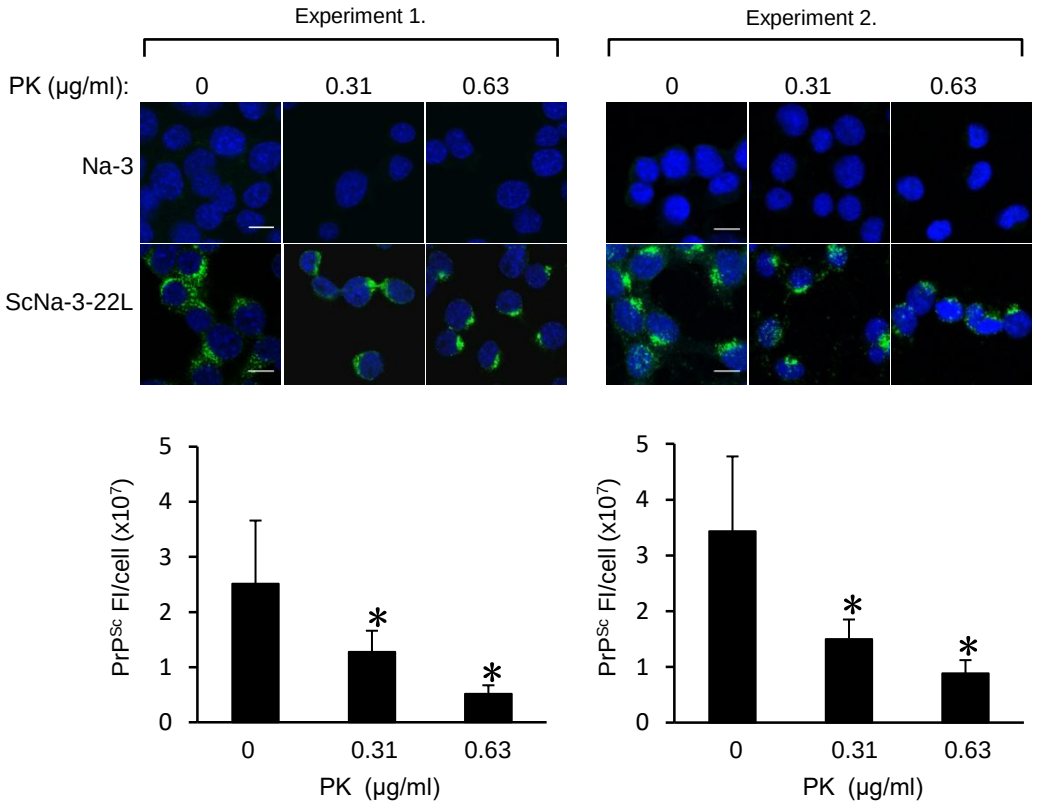

Figure I-6. Possible detection of PrP^{Sc}-sen and PrP^{Sc}-res using mAb 132 in IFA.
N2a and ScN2a-3-22L cells and were cultured in a chambered coverglass for 24 h. Cells were fixed with 4% paraformaldehyde in PBS for 10 min and then treated with 0.1% Triton X-100 and 0.1 M glycine in PBS. Subsequently, cells were treated with PK at the indicated concentrations at 4 ° C for 30 min. Cells were then treated with 5 M GdnSCN for 10 min at r.t. and subjected to PrP^{Sc}-specific immunofluorescence staining. Representative fluorescence images of two independent experiments are shown at the top. Graphs show the corresponding quantification result of PrP^{Sc} fluorescence intensities (FI) per ScN2a-3-22L cell. Fluorescence intensities from perinuclear regions of N2a-3 were subtracted as background. Experiment 1: mean fluorescence intensities and standard deviations of 16 cells from five microscopic fields (3–4 cells/field). Experiment 2: mean fluorescence intensities and standard deviations of 16–24 cells from four to five microscopic fields (3–5 cells/field). *, $p < 0.001$ (Welch's *t*-test). Scale bars: 10 μm.

molecule. However, mAb 132 did not show a positive reaction to uninfected cells, even after GdnSCN treatment. I do not have any clear explanation for this phenomenon, one possibility is that once the region containing containing the mAb 132 epitope on PrP^{C} was exposed by GdnSCN treatment, the region may refold into antibody-inaccessible form after the removal of GdnSCN. Surface plasmon resonance analysis revealed that the binding of monovalent mAb132 (e.g., recombinant Fab) was significantly weaker than bivalent mAb 132 (e.g., recombinant IgG), indicating that the bivalent binding is required for the efficient binding to the epitope (Akio Suzuki & Motohiro Horiuchi., manuscript in preparation). Reaction of mAb 132 to PrP^{C} expressed in the cells will be a monovalent binding, whereas that to PrP^{Sc} will occur as bivalent binding because PrP^{Sc} exists as oligomer/aggregate of PrP molecules. Thus the binding kinetics of mAb 132 may partly explain the inefficient binding of mAb 132 to PrP^{C}: monovalent binding is not enough to stain PrP^{C} efficiently in IFA. However, further studies are still required for the elucidation of the mechanism of PrP^{Sc}-specific staining by mAb 132.

Conformation-dependent immunoassay (CDI) has demonstrated the existence of PrP^{Sc}-sen and PrP^{Sc}-res in the brains of prion-affected humans and animals (Safar *et al.*, 1998). The proportion of PrP^{Sc}-sen is believed to be high; for example, CDI revealed that PrP^{Sc}-sen constituted approximately 50–90% and 90% of PrP^{Sc} in the brains of hamsters infected with hamster-adapted prion strains and CJD patients, respectively (Safar *et al.*, 1998; Safar *et al.*, 2005). Also immuno-electron microscopic analysis of mice infected with the RML strain let to an estimate that >85% of the PrP^{Sc} in the brain was PK-sensitive (Godsave *et al.*, 2008). The PK-sensitive fraction of PrP^{Sc} is reported to possess higher infectivity and higher conversion activity per PrP molecule than the PK-resistant fraction (Silveira *et al.*, 2005). Taken together,

these results suggest that PrP^{Sc}-sen may be the more substantial entity of prions. Thus, evaluation of the effect of compounds on PrP^{Sc}-sen may be important for screening anti-prion compounds. Screening methods of anti-prion compounds using prion-infected cells reported to date included PK treatment for the removal of PrP^{C} (Ghaemmaghami *et al.*, 2010; Heal *et al.*, 2007; Kocisko *et al.*, 2003; Leidel *et al.*, 2011). However, effect of compounds on PrP^{Sc}-sen cannot be assessed or may be underestimated if PK treatment is included during the analysis.

MAb 132 discriminated PrP^{Sc} from PrP^{C} without PK treatment, suggesting that mAb could detect both PrP^{Sc}-sen and PrP^{Sc}-res (Sakai *et al.*, 2013; Yamasaki *et al.*, 2014b; Yamasaki *et al.*, 2012); however, this had not yet been directly demonstrated. In a dot-blot analysis performed using cell lysates prepared with non-ionic detergent, the PrP^{Sc} level detected after PK digestion and subsequent GdnSCN treatment was much lower than that detected after GdnSCN treatment alone (Fig. I-5). Consistent with the result of dot-blot analysis, the fluorescence intensities of PrP^{Sc} decreased after treatment of the cells with even low concentrations of PK (Fig. I-6). Quantification of the result of dot-blot analysis and the IFA implies that >50% of PrP^{Sc} in N2a-3 cells infected with the 22L strain are sensitive to PK, which is similar to the proportion of PK-sensitive PrP^{Sc} in the brains of prion-affected humans and animals (Cronier *et al.*, 2008; Safar *et al.*, 1998; Safar *et al.*, 2005). Taken together, these results demonstrate that mAb 132 detects not only PrP^{Sc}-res, but at least a certain fraction of PrP^{Sc}-sen if not all.

The absolute sensitivity for the detection of PrP^{Sc} in the cell-based ELISA is not expected to be high because of the lack of procedures for PrP^{Sc} concentration such as phosphotungstic acid precipitation (Ghaemmaghami *et al.*, 2010; Wadsworth *et al.*, 2001).

However, a 1 log dynamic range for direct PrP^{Sc} detection in prion-infected cells is enough to evaluate the anti-prion effect exerted by a 50% effective dose as a primary screening method. The remarkable advantage of the cell-based ELISA is its simplicity: all the procedures, from cell culture to PrP^{Sc} detection, can be completed in the same plate without making cell lysates or PK treatment. Probing both PrP^{Sc}-res and PrP^{Sc}-sen is another technical improvement, which is difficult to achieve using procedures that include PK treatment. It is believed that human cells or human PrP^{C}-expressing cells infected with human prions are a better platform for screening for potential therapeutic reagents than prion-infected cells of other species. The epitope for mAb 132 is well conserved from mammals to chickens (Ishiguro *et al.*, 2009; Wopfner *et al.*, 1999), so mAb 132 will be applicable to the detection of PrP^{Sc} from human prion-infected cells using a protocol similar to the one developed in this study.

BRIEF SUMMARY

Prion-infected cells have been used for analyzing the effect of compounds on the formation of abnormal isoform of prion protein (PrP^{Sc}). PrP^{Sc} is usually detected using anti-prion protein (PrP) antibodies after the removal of the cellular isoform of prion protein (PrP^{C}) by proteinase K (PK) treatment. However, it is expected that the PK-sensitive PrP^{Sc} (PrP^{Sc}-sen), which possesses higher infectivity and conversion activity than the PK-resistant PrP^{Sc} (PrP^{Sc}-res), is also digested through PK treatment. To overcome this problem, I established a novel cell-based ELISA in which PrP^{Sc} can be directly detected from cells persistently infected with prions using anti-PrP monoclonal antibody (mAb) 132 that recognizes epitope consisting of mouse PrP amino acids 119–127. The novel cell-based ELISA could distinguish prion-infected cells from prion-uninfected cells without cell lysis and PK treatment. MAb 132 could detect both PrP^{Sc}-sen and PrP^{Sc}-res even if all PrP^{Sc} molecules were not detected. The analytical dynamic range for PrP^{Sc} detection was approximately 1 log. The coefficient of variation and signal-to-background ratio were 7%–11% and 2.5–3.3, respectively, demonstrating the reproducibility of this assay. The addition of a cytotoxicity assay immediately before PrP^{Sc} detection did not affect the following PrP^{Sc} detection. Thus, all the procedures including cell culture, cytotoxicity assay, and PrP^{Sc} detection were completed in the same plate. The simplicity and non-requirement for cell lysis or PK treatment are advantages for the high throughput screening of anti-prion compounds.

Chapter II

Therapeutic effect of an autologous compact bone derived mesenchymal stem cell transplantation on prion disease

INTRODUCTION

In the Chapter I, I established a novel cell-based ELISA for the screening of anti-prion compounds. In addition to the inhibition of PrP^{Sc} formation, the protection of neurons or regeneration of degenerated neurons is also thought to be important in the treatment of prion diseases. Previously, my laboratory reported that intracerebral or intravenous transplantation of immortalized human bone marrow-derived MSCs (BM-MSCs) prolonged the survival of mice infected with prions. The transplanted BM-MSCs were migrated to brain lesions and produced neurotrophic factors such as brain-derived neurotrophic factors (BDNF), vascular endothelial growth factor (VEGF), neurotrophin 3 and 4/5 (Song *et al.*, 2009). Furthermore, human BM-MSCs differentiated into neuron-, astrocyte-, or oligodendrocyte-like cells in the brains of prion-infected mice. These results suggested the neuroprotective effects of human BM-MSCs in prion disease. However, those experiments were allogenic transplantation and thus not human BM-MSCs themselves but human PrP^{C} expressed in human BM-MSCs might impede prion propagation in mouse brain by the interference of intermolecular interaction between mouse PrP^{C} and PrP^{Sc} (Horiuchi *et al.*, 2000; Priola & Caughey, 1994; Prusiner *et al.*, 1990). Alternatively, immortalized human BM-MSCs that could proliferate more efficiently than primary MSCs are expected to exist a longer period in the brain lesions might result in overestimation of the effect.

Therefore, to evaluate the effect of autologous MSCs transplantation on prion disease, in this study, I isolated MSCs from compact bone from mouse femur and tibia, and analyzed therapeutic potential of compact-bone derived MSCs (CB-MSCs) on prion disease.

MATERIALS & METHODS

Prion inoculation

All animal experiments were performed according to protocols approved by the Institutional Committee for Animal Experiments. Four-week-old female ICR mice were purchased from CLEA Japan, Inc. (Japan), and the mice were acclimatized for a week prior to use. Mice were intracerebrally inoculated with 20 μl of 2.5% brain homogenates from Jcl:ICR mice infected with Chandler strain at the terminal stage of the disease. Mock-infected group of mice were intracerebally inoculated with 20 μl of 2.5% brain homogenates from age-matched uninfected Jcl:ICR mice. All mice were maintained on *ad libitum* feed and water with a 12-h light/dark cycle.

Isolation of MSCs from mouse compact bone

Six-week-old Jcl:ICR female mice were euthanized under anesthesia with SEVOFRANE (Maruishi Pharmaceutical Company). The femur and tibia were obtained for the isolation of CB-MSCs (Zhu *et al.,* 2010). Both ends of femur and tibia were cut by scissors and bone marrow was washed out with Hanks' Balanced Salt Solution (HBSS, Sigma) by inserting the 27 G needle (Terumo) into the cavity. Then femur and tibia were cut into small pieces by bone scissors. After washing with HBSS, the bone fragments were digested with 1 mg/ml collagenase II (Sigma) in HBSS with constant shaking at 220 rpm for 2 h at 37 ℃. The digest was filtered through a 100 μm cell strainer (BD Falcon) and the remaining bone fragments on the cell strainer were washed three times with HBSS. The bone fragments

were cultured with Dulbecco's Modified Eagle Medium (DMEM, Sigma) containing 10% fetal bovine serum (FBS, Gibco), 10% horse serum (Gibco), 2 mM L-glutamine (Wako), 10 mM HEPES (Gibco) and 100 U/ml Penicillin-Streptomycin (PS, Gibco) (FBS-HS-DMEM) in 10 cm plates. The filtrated cells were also cultured with FBS-HS-DMEM in 10 cm plates at 37 ℃ under 5% CO_2 and 5% O_2. Cells were freshly fed everyday in the first 3 days, then passaged every 3 to 4 days.

Purification of CB-MSCs by Magnetic Activated Cell Sorting (MACS)

Compact bone-derived cells adhered to plastic plate was harvested with 0.1% collagenase I (Wako) in PBS when the cells were reached to about 70% confluent. The cells were collected by centrifugation and incubated with 200 μl CD11b microbeads (Miltenyi Biotec) diluted at 1 : 10 with HBSS containing 0.5% FBS (0.5% FBS-HBSS) for 15 min on ice. Then CD11b-positive cells were removed by passing through MS Column set on MACS Separators (Miltenyi Biotec), and the pass through fraction was collected. The collected cells were subsequently incubated with 200 μl CD 45 microbeads (Miltenyi Biotec) diluted at 1:10 with 0.5% FBS-HBSS for 15 min. CD45-positive cells were removed by the MS Column set on MACS Separators. Cells in the pass through fraction were cultured as CB-MSCs.

Flow cytometric analysis

The CB-MSCs were harvested with collagenase treatment and suspended with 0.5% FBS-HBSS. The CB-MSCs were added to 96-well plates (1×10^5 cells/well). After centrifugation, cells were incubated with 100 μl primary rat antibodies against mouse CD11b, CD45, CD29, CD44, CD73, CD90.2, CD105, CD106, Sca-1 and CD140a at a 1:200 dilution

for 30 min on ice. All the antibodies except for anti-CD73 antibody were purchased from Biolegend. Anti-CD73 antibody was purchased from BD Bioscience. Rat IgG2a kappa and IgG2b kappa, both from Biolegend, were used as isotype controls. The cells were washed 3 times with 0.5% FBS-HBSS and incubated with anti-rat Alexa Fluor 488 (Molecular Probes) at a 1 : 1,000 dilution for 30 min on ice. After washing three times with 0.5% FBS-HBSS, the cells were stained with 5 μg/ml of propidium iodide (Molecular Probes) in HBSS for 5 min. The cells were analyzed using FACSVerse flow cytometer (BD Biosciences).

Transplantation of CB-MSCs

For transplantation of CB-MSCs into hippocampus, mice were anesthetized by intramuscular injection of xylazine (10 mg/kg) and ketamine (50 mg/kg) and were placed on a stereotaxic apparatus (Narishige, Japan). After a linear scalp incision, burr holes were drilled to accommodate stereotaxic placement into the left hippocampus (2.0 mm caudal; 2.0 mm lateral to the bregma. CB-MSCs (1×10^5 cells in 2 μl PBS) were transplanted over a period of 15 min using a Hamilton syringe with a 31-gauge needle set in a micromanipulator. Two microlitters of PBS was injected into the same position as the sham-operation.

Immunoblotting

Brains were sagittally hemi-sectioned and homogenized in 20% (w/v) TMS buffer [10 mM Tris-HCl (pH 7.5), 5 mM $MgCl_2$, 5% Glucose]. The 20% brain homogenate (250 μl) was mixed with an equal volume of a detergent buffer [8% Zwittergent 3-14, 1% Sarcosyl, 100 mM NaCl, and 50 mM Tris-HCl (pH 7.5)] and digested with collagenase I at 0.5 mg/ml for 15 min at 37℃ in water bath. To detect PK-resistant PrP^{Sc}, the samples were digested with PK

(Roche) at 20 μg/ml for 30 min at 37 ℃ in water bath. After stopping PK digestion by adding Pefabloc (Roche) to 2 mM, DNase I was added to the samples at 40 μg/ml and incubated 5 min at r.t. A half volume of butanol-methanol solution (2-butanol : methanol = 5 : 1) was added and PK-resistant PrP^{Sc} was recovered by centrifugation at 15,000 rpm for 10 min at 20 ℃. The resulting pellet was dissolved in 1 × SDS sample buffer [62.5 mM Tris-HCl (pH 6.8), 5% glycerol, 3 mM EDTA, 5% SDS, 4 M Urea, 0.04% bromophenol blue, 4% β-mercaptoethanol] by boiling for 5 min. To detect total PrP, PK digestion and Pefabloc treatment were omitted. SDS-PAGE and immunoblotting for PrP^{Sc} detection were carried out as described in Chapter I.

Histopathology and immunohistochemistry

Mice were dissected under anesthesia and brains were fixed with 10% formalin (Wako), soaked into 60% fomic acid (Wako) for 1 h and then kept in 70% ethanol (Wako). After embedded in paraffin, the samples were cut into sections (3 μm). The sections were deparaffinized, rehydrated and subjected to haematoxylin-eosin (HE) staining or immunohistochemistry. For HE staining, sections were stained in haematoxylin (Wako) for 3 min and washed with tap-water for 5 min and then washed again with de-ionized water (DW). After the pre-treatment with 95% of ethanol, sections were stained with 0.5% eosin (Wako) for 2 min and dehydrated by a series of ethanol. The sections were permeabilized against xylene (Wako) and enclosed with cover glass using Mount-Quick (Daido Sangyo).

To detect PrP^{Sc} by immunohistochemistry, sections were autoclaved for 20 min at 135 ℃ (Furuoka *et al.*, 2005). The sections were treated with 3% H_2O_2 in methanol for 15 min, blocked with 5% FBS in PBS for 30 min and then incubated with mAb 31C6 (0.5 μg/ml) for 1

h at 37℃. After washing with PBST, the sections were incubated with Envision+ system-HRP labelled polymer conjugated to goat anti-mouse immunoglobulins (Dako) for 1 h at 37℃. The sections were washed with PBST and developed with DAB Peroxidase (Vector), followed by counterstaining with Mayer's haematoxylin.

To detect glial fibrillary acidic protein (GFAP) and ionized calcium binding adaptor molecule 1 (Iba-1), markers for activated astoryctes and microglia, respectively, sections were treated with 500W microwave in citric acid buffer [0.01M citric acid and 0.01M sodium citrate] for 5 min twice for antigen retrieval (Furuoka *et al.*, 2005). Then sections were treated with 0.3% of H_2O_2 and blocked with FBS as described above. After blocking, the sections were incubated with anti-GFAP (Dako) at 1:2,000 or anti-Iba-1 (Wako) at 1:200 dilution for 1 h at 37℃. After washing with PBST, the sections were incubated with EnVision+ system-HRP labelled polymer conjugated to goat anti-rabbit immunoglobulins (Dako) for 1 h at 37℃. The sections were then developed and counterstained as described above.

Migration assay

Brains of the Chandler strain-infected mice at 120 days post inoculation (dpi), or of age-matched mock-infected mice, were homogenized to 20% (w/w) in DMEM. The homogenates were centrifuged at 10,000 × *g* for 10 min at 4°C, and the resulting supernatants were passed through a 0.22-μm pore size filter. Aliquots of the brain extracts were stored at –80℃ until use. The CB-MSCs that were starved in serum-free DMEM for 24 h were harvested with 0.1% collagenase I. Wells of the 24-well plate were supplied with serum-free DMEM containing brain extracts, and CB-MSC suspensions (5×10^4 cells with 400 μl of DMEM) were added to the insert well with the polycarbonate membrane (24-well Millicell

Hanging Cell Culture Inserts, pore size, 8.0 μm). The 24-well plate set with the insert wells were incubated for 16 h at 37 ℃. The CB-MSCs on the polycarbonate membrane were stained with 1% crystal violet in methanol for 1 h on ice. After washing with de-ionized water, non-migratory cells that stayed on the upper side of the polycarbonate membrane were removed using a cotton swab. The migrated CB-MSCs, which had passed through the pores and clung to the underside of the membrane were observed with BIOREVO BZ-9000 microscope (Keyence), and the cell numbers were counted using the NIH Image J Program.

Quantitative reverse transcription-polymerase chain reaction (qRT-PCR)

After collected mice brains, hippocampus were isolated under the microscope and total RNA was extracted using TRIzol Reagent (Life Technologies). First-strand cDNA was synthesized from 1 μg of the total RNA using the First Strand cDNA Synthesis Kit (GE Healthcare). The amplification reaction mixtures contained the cDNA synthesis reaction mixture diluted (2 μl, 1:8 by deionized water unless otherwise), predesigned TaqMan Gene Expression Assays (0.5 μl), and 2 × TaqMan Fast Universal PCR Master Mix (5 μl) in the final reaction volume of 10 μl. TaqMan Gene Expression Assay (Applied Biosystems) used were as follows: mouse Iba-1 (*Aif1*, Mm 00479862-g1), *CD68* (Mm 00839636), *Ym1* (*Chi3l3*, Mm 00657889-mH), *Fizz1* (*Retnla*, Mm00445109-m1), *Mrc1* (Mm 00485148-m1), *IL-10* (Mm 99999062-m1), *TNF-α* (Mm 00443258-m1), *IL-1β* (Mm 01336189-m1), *BDNF* (Mm 04230607-s1), *NGF* (Mm 00443039-m1). The expression of mouse β-actin gene was analyzed using Mouse ACTB (4352933E, Applied Biosystems) and used for normalization. TaqMan assays were carried out using 7900HT Fast Real-Time PCR system (Life Technologies). Results were analyzed by comparative cycle threshold (2-ΔΔct) method to calculate fold

changes.

Statistical analysis

Statistical analysis was done with the JMP Pro 12.2.0 statistical software (SAS Institute).

RESULTS

Expression of cell surface markers on CB-MSCs

After removing CD11b- and CD 45-positive cells by MACS, CB-MSCs were serially passaged to expand cell numbers. At the 4^{th} passage, expression of surface markers was analyzed by flow cytometry (Fig. II-1). The cells were negative for myeloid-derived markers CD11b and CD45, but molecules that are reported to be expressed on the surface of MSCs, CD29, CD44, CD73, CD90.2, CD105 and Sca-1(Dominici *et al.*, 2006; Pittenger *et al.*, 1999), CD106 (Ren *et al.*, 2010; Yang *et al.*, 2013), and CD140a (Morikawa *et al.*, 2009), were expressed on the surface of CB-MSCs. However, the histogram of CD73, CD90.2, CD105, and CD106 showed that CB-MSCs included cells that were positive and negative for these molecules, indicating that CB-MSCs are composed of heterologous cell population.

Migration of CB-MSCs to brain extract

MSCs are known to migrate brain lesions of animal models of neurodegenerative disorders, such as Parkinson's disease (Hellmann *et al.*, 2006), ischemia (Chen *et al.*, 2001), glioma (Nakamura *et al.*, 2004), and brain tumor (Kim *et al.*, 2016). My laboratory has

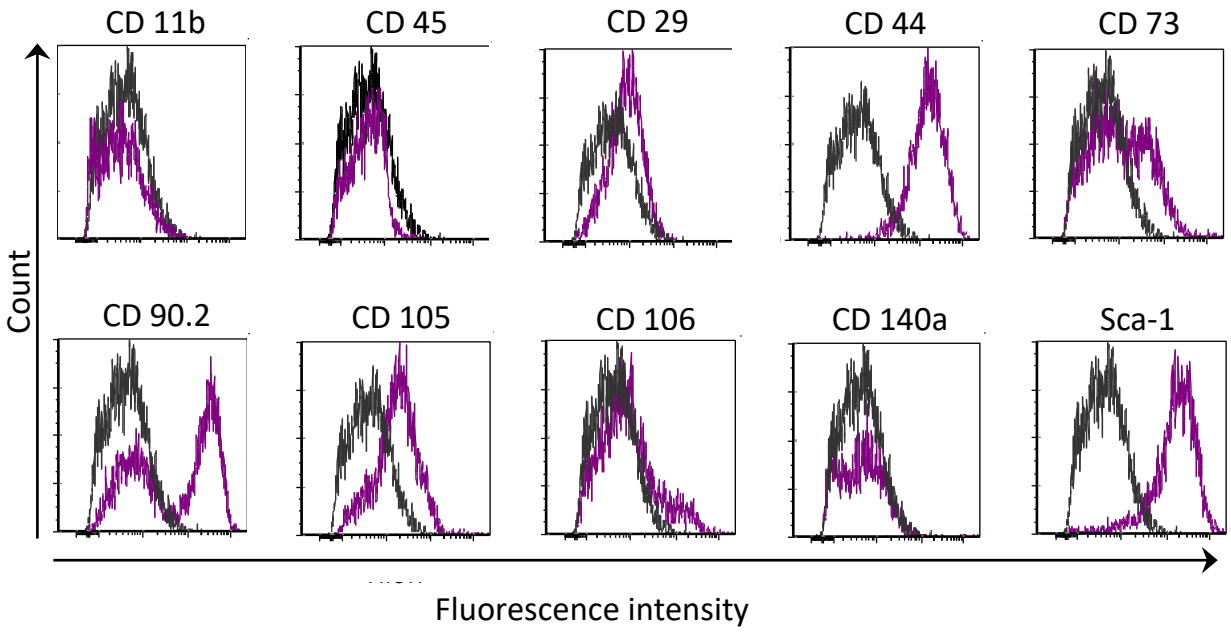

Figure II-1. Expression of surface markers on CB-MSCs cells.
Compact bone-derived cells that adhered to plastic plate were purified by MACS to removed CD11b- and CD45-positive cells and analyzed by flow cytometry. The expression of surface markers on CB-MSCs was analyzed at the 4th passage (purple lines) and the black lines show the histogram of corresponding isotype control antibody.

reported that the immortalized human BM-MSCs transplanted intracerebrally or intravenously migrate to brain lesions of prion disease (Song *et al.*, 2009). The human BM-MSCs also migrated to brain extracts from mice infected with prions *in vitro* migration assay, indicating that capability of BM-MSCs in migrating to lesions of prion disease *in vivo* will be assessed by the *in vitro* migration assay (Song *et al.*, 2011). Thus, the migration ability of CB-MSCs to brain extracts from the Chandler strain-infected mice was assessed using the *in vitro* migration assay (Fig. II-2). Figure II-2A shows CB-MSCs migrated to the bottom side of the insert wells. Quantitative analysis of the migrated CB-MSCs revealed that 3.0 and 2.1 times as many CB-MSCs migrated to 1% and 0.1% brain extracts from prion-infected mice, respectively, than to those of corresponding uninfected mice (Fig. II-2B).

Effect of CB-MSCs on survival of prion-infected mice

The result of migration assay suggested that CB-MSCs are capable of migration to lesion of prion disease. Thus I examined whether the transplantation of CB-MSCs ameliorates prion disease. CB-MSCs were transplanted into the left hippocampus of the Chandler strain infected mice at 120 dpi. The intra-hippocampal transplantation of CB-MSCs prolonged the survival of mice infected with the Chandler strain (163.8 ± 6.2 days, n = 9) over that of PBS injected group (155.0 ± 2.4 days, n = 7) (Fig. II-3A, $p<0.05$)

Loss of body weight with disease progression is one of the prominent features in the Chandler strain-infected mice (Ohsawa *et al.*, 2013; Song *et al.*, 2008). To evaluate the effect of CB-MSCs on disease progression using more objective parameter, I weighed the mice every week after 120 dpi. At 141 dpi, the decrease in body weight appeared to slow down in CB-MSCs transplanted group compared with PBS injected group (Fig. II-3B, $p<0.05$), and

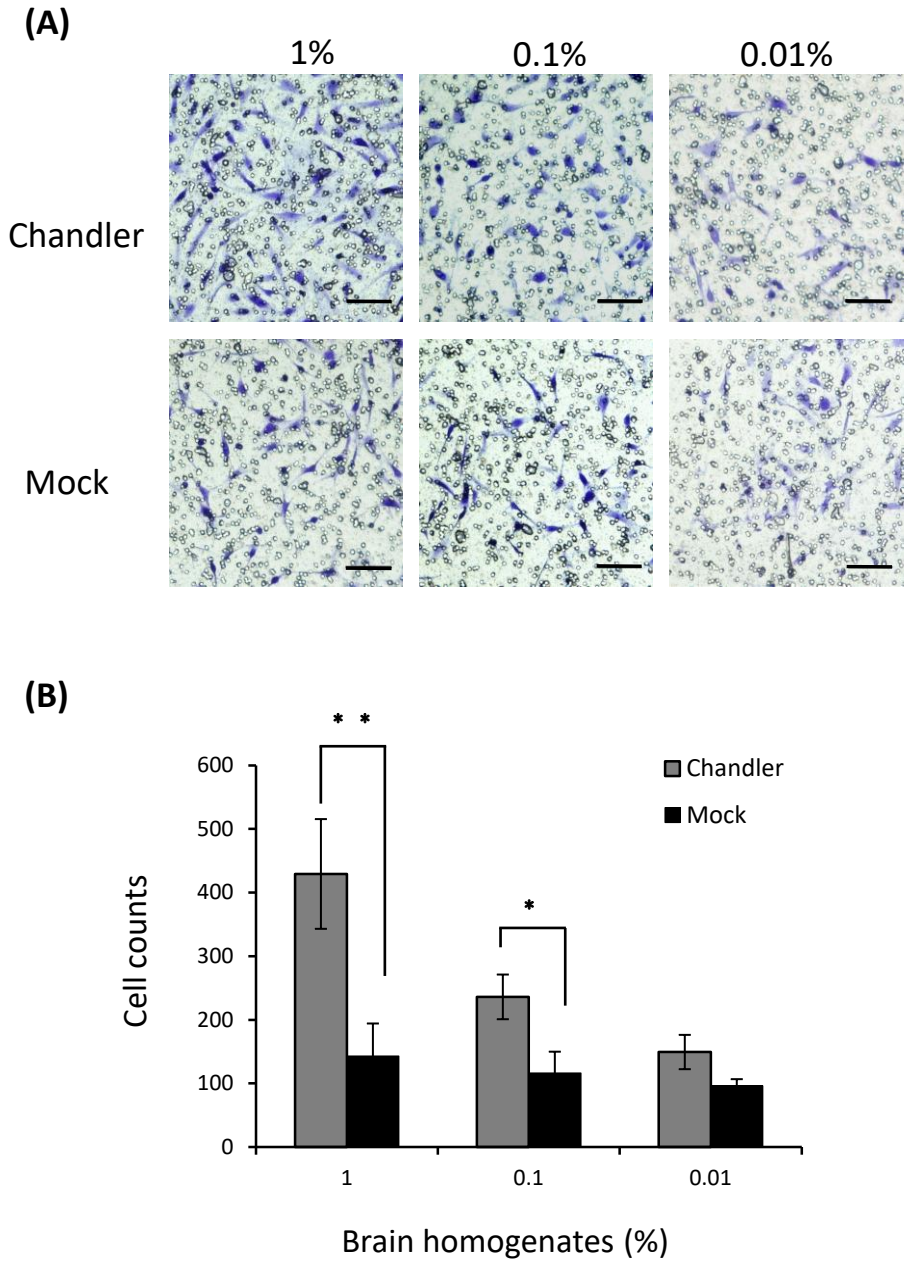

Figure II-2. Migration of CB-MSCs to brain extracts from prion-infected mice.
Insert wells containing pre-starved CB-MSC suspension (5×10^4 cells) were placed in the wells of 24-well plate that contained serum-free DMEM with 1%, 0.1% or 0.01% brain extracts of the Chandler strain- or mock-infected mice and were incubated for 16 h. The membranes of insert wells were stained with crystal violet. (A) Migrated CB-MSCs clung to the underside of the membrane. Bars = 100 μm. (B) Numbers of CB-MSCs migrated to brain extracts from the Chandler strain or mock-infected mice. The stains that are larger than 2×10^2 μm^2 were counted as cells. Means and standard deviations (SD) from a total of 10 areas (1.20×10^6 μm^2/area) of 2 wells (5 areas per each well) are shown. The graphs show cell counts per 1.20×10^6 μm^2/area. *, $p < 0.05$; **, $p<0.01$(Student's *t*-test).

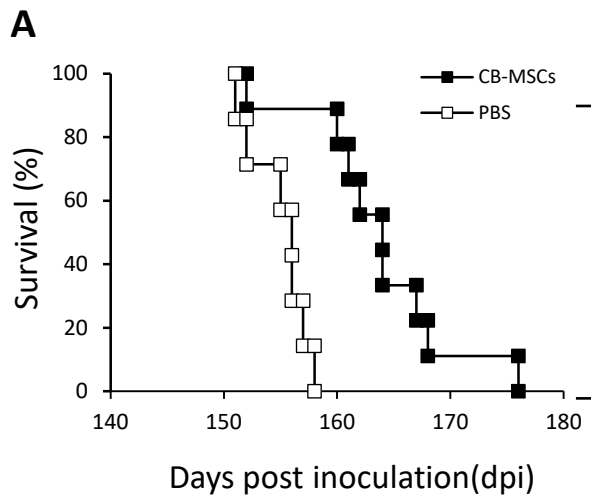

Intra-hippocampus injection	N	Survival time (days)	Mean ± SD
CB-MSCs	9	152, 160, 161, 162, 164, 164, 167, 168, 176	163.8 ± 6.2 *
PBS	7	151, 152, 155, 156, 156, 157, 158	155.0 ± 2.4

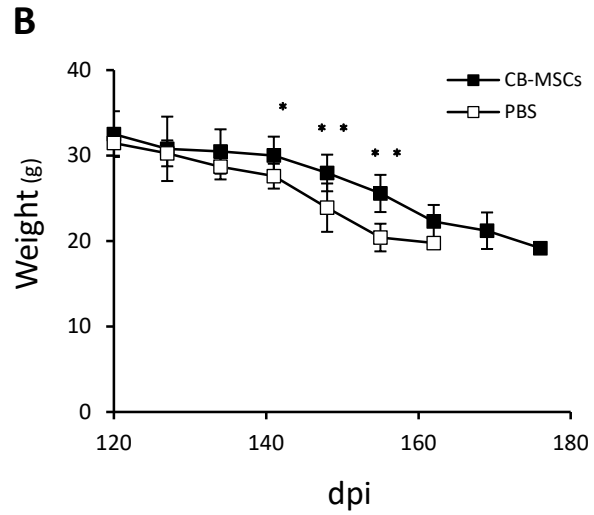

Figure II-3. Effect of CB-MSCs on the survival of mice infected with the Chandler prion strain.

(A) Survival curves and survival periods of individual mouse. CB-MSCs (1×10^5 cells in 2 μl PBS) were transplanted to the Chandler strain-infected mice at 120 dpi (n = 9, closed square). As a sham-operation group, the same volume of PBS was injected to the Chandler strain-infected mice at 120 dpi (n = 7, open square). The X-axis indicates the survival time after prion inoculation, and the Y-axis indicates survival rate (%). The table on the right shows the survival time of individual mouse in each group. *, $p < 0.05$ (*Kaplan-Meier* survival estimates, *Wilcoxon* signed-rank tests). (B) Changes in body weight. After the transplantations of CB-MSCs, mice were weighed weekly up to the terminal stage of the disease. Graph shows mean weight ± SD. *, $p < 0.05$; **, $p < 0.01$ (Two-way ANOVA with *post hoc* Bonferroni tests).

differences in body weight were more obvious at 148 and 155 dpi (Fig. II-3B, $p<0.01$).

Effect of CB-MSCs on PrP^{Sc} accumulation and neuropathology

To analyze whether CB-MSCs influence PrP^{Sc} accumulation in the brain, I transplanted CB-MSCs to hippocampus of the Chandler-infected mice at 120 dpi and kinetics of a total PrP and proteinase K-resistant PrP (PrP^{Sc}) levels were analyzed by immunoblotting (Fig. II-4). At 145 dpi, the mean PrP^{Sc} level of the PBS-injected group increased nearly 2-fold over the level at 120 dpi; however, no difference was observed in the PrP^{Sc} levels of CB-MSCs transplanted and PBS-injected groups. PrP^{Sc} levels were further increased at the terminal stage of the disease, however, no difference was observed in the PrP^{Sc} levels between CB-MSCs transplanted and PBS-injected groups (Figs. II-4A & II-4C). The mean total PrP level of the CB-MSCs transplanted group increased 1.3- and 1.8-fold at 145 dpi and at the terminal stage, respectively, compared with the levels at 120 dpi; however, no difference in the total PrP levels were observed between CB-MSCs transplanted group and PBS-injected group (Figs. II-4B & II-4D). These results indicated that CB-MSCs did not influence the accumulation of PrP^{Sc} in brains. Being consistent with the results of PrP^{Sc} accumulation by immunoblotting, no obvious difference was observed in PrP^{Sc} accumulation in the hippocampus and thalamus of CB-MSCs transplanted and PBS-injected groups by immunohistochemistry for PrP^{Sc} at 145 dpi and at the terminal stage (Fig. II-5A, PrP^{Sc}). No difference was observed in the astrogliosis in the hippocampus and thalamus of CB-MSCs transplanted and PBS-injected groups by immunohistochemistry for GFAP (Fig. II-5A, GFAP). In contrast, there was difference in microglial activation (Fig. II-5A, Iba-1): quantitative analysis revealed that Iba-1 positive cells were more in CB-MSCs transplanted group than in PBS-injected group in hippocampus at 145 dpi (Fig. II-5B, $p<0.05$). However, no difference in the number of

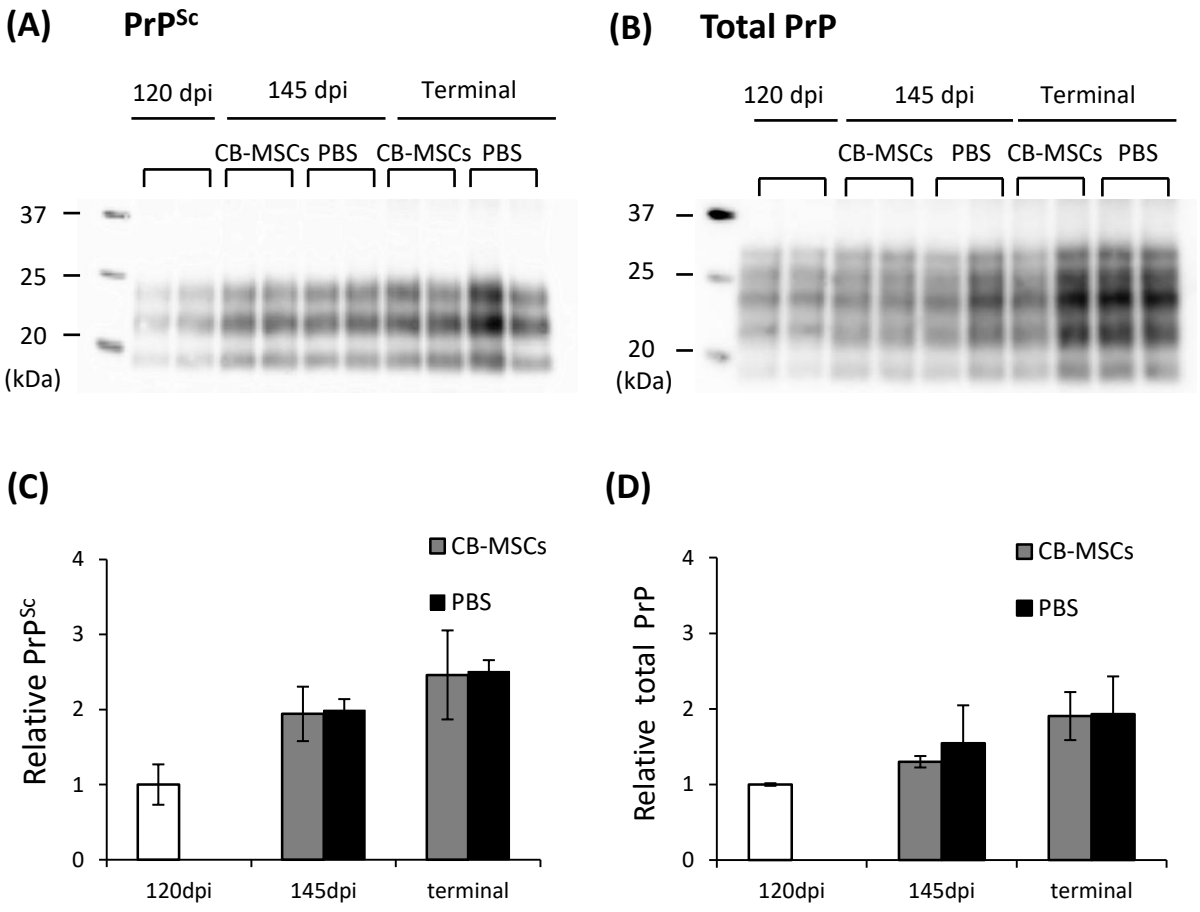

Figure II-4. Detection of PrP^{Sc} and total PrP in brain homogenates.
In one experiment, a total of 10 mice infected with the Chandler strain were used. Two of the mice were sacrificed at 120 dpi. The remaining mice were divided into two groups; 4 mice were transplanted with CB-MSCs and the remaining 4 were injected with PBS as sham operation. At 145 dpi (25 days after transplantation), two mice from the CB-MSCs transplanted group and PBS injected group were sacrificed and the remaining 2 mice in each group were sacrificed at the terminal stage of the disease. The left half of the brains were collected and used for detection of PrP^{Sc} and total PrP by immunoblotting, whereas the right hemispheres were used for histopathological examinations in Fig. II-5. (A and B) samples (10 μl, 100 μg brain equivalent) were loaded onto each well, and detection of PrP^{Sc} and total PrP. PrP^{Sc} (A) and total PrP (B) at 120 dpi, 145dpi and at the terminal stage (CB-MSCs transplanted group, 161 and 168 dpi; PBS injected group, 156 and 158 dpi). PrP^{Sc} and total PrP were detected using anti-PrP mAb 31C6. Molecular mass markers are shown at left. (C and D) Relative levels of total PrP^{Sc} (C) and PrP (D). The same size of an independent experiment was carried out and the results of a total of four mice at each time point were quantified. Mean levels ± SD PrP^{Sc} and total PrP relative to those at 120 dpi are indicated.

microglia was observed at the terminal stage of the disease. No difference was observed in the vacuolation in the hippocampus or thalamus of CB-MSCs transplanted and PBS-injected groups (Fig. II-5A, HE & Fig. II-5C).

To analyze the activation state of microglia, qRT-PCR was carried out (Fig. II-6). The expression of *Aif1* gene that encodes Iba-1, was up-regulated in prion-infected mice; however, further up-regulation of *Aif1* gene was observed in prion-infected mice transplanted with CB-MSCs compared with those with sham operation. No difference was observed in *Aif1* gene expression in mock-infected mice transplanted with CB-MSCs and those with sham operation. The expression of *CD68*, which is used as a marker for activated microglia, was also significantly up-regulated more in prion-infected mice transplanted with CB-MSCs than those with sham operation. The expression of *IL-1β*, representative pro-inflammatory cytokine, was up-regulated upon prion infection (compare Mock PBS vs Chandler PBS) as reported; however interestingly, further significant up-regulation was observed in prion-infected mice transplanted with CB-MSCs. The expression of other pro-inflammatory cytokine gene, *TNF-α*, showed the similar tendency. No significant difference was found in *BDNF* and *NGF* gene expression in the four groups (Chandler MSC vs Chandler PBS vs Mock MSCs vs Mock PBS). Concerning some of the marker genes for M2-type activation in macrophages, *Ym1* and *Fizz1*, CB-MSCs transplantation did not influence their gene expressions in mock-infected mice; however, the gene expression was remarkably up-regulated in prion-infected mice transplanted with CB-MSCs. These suggest that the transplantation of CB-MSCs influenced the activation state of microglia in prion-infected mice. The gene expression of *IL-10*, anti-inflammatory cytokine that stimulates microglia to shift M2-type activation state, was markedly up-regulated by CB-MSCs transplantation in mock-infected mice, although the degree of up-regulation was smaller than that observed in

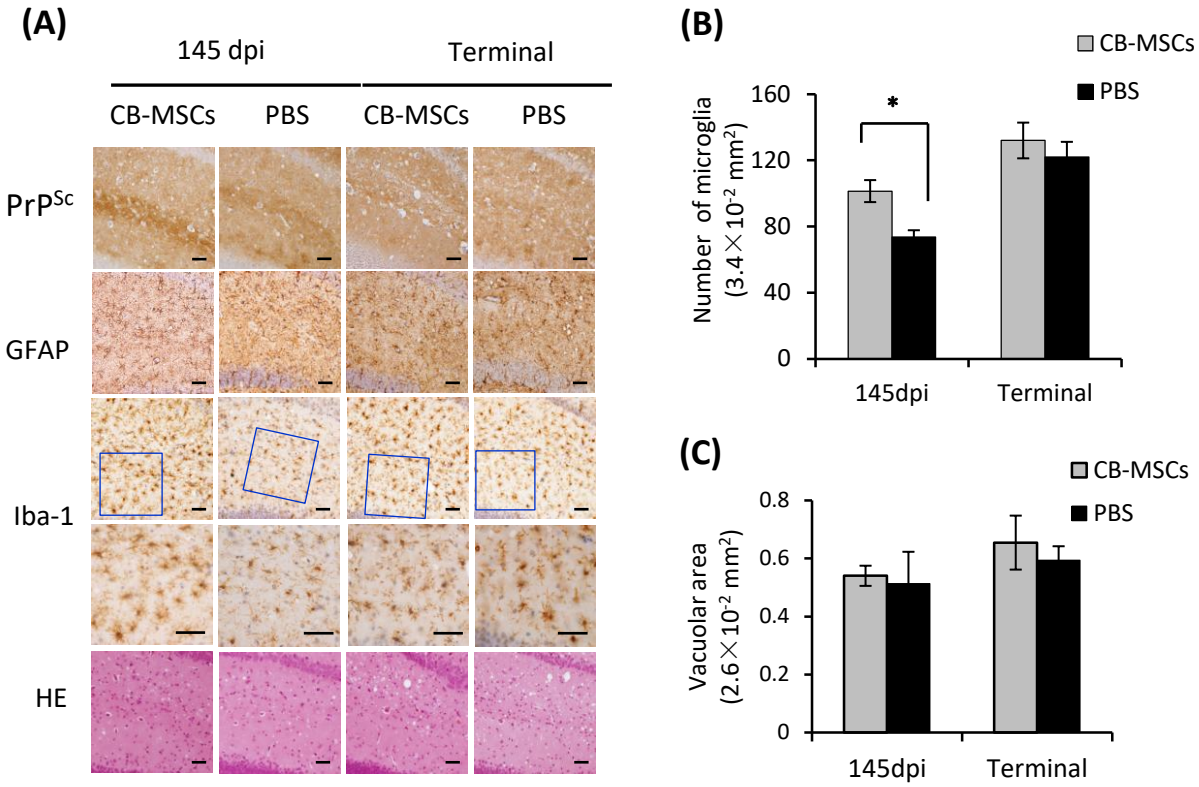

Figure II-5. Effects of intra-hippocampus transplantation of CB-MSCs on neurohistopathological changes.

The right hemispheres of mice described in Fig. II-4 were fixed with 10% formalin for histopathological examination. Paraffin-embedded sections were subjected to immunohistochemical analysis for PrP^{Sc} using mAb 31C6, astrocytes using anti-GFAP antibody, microglia using anti-Iba-1 antibody and hematoxylin and eosin (HE) staining. (A) Immunohistochemistry and HE staining of hippocampus at 145 dpi and the terminal stage of the disease. The microglia in the region of interest (blue squares) in Iba-1 stained sections were magnified and showed under each original section. Bars = 20 μm. (B) Numbers of microglia in hippocampus. Iba-1-positive microglia in sections were counted by Image J. Stains larger than 10 μm^2 were count as cells. Means and SD from a total of 15 areas (3.4×10^{-2} mm^2/area, 5 areas per one section from each mouse, three mice) are shown. (C) Quantitative analysis of vacuolar regions in hippocampus. Vacuolar regions in HE stained sections were quantified by Image J. Stains with between 20 μm^2 to 30 μm^2 were measured as vacuolar regions. Means and SD from 3 areas (2.6×10^{-2} mm^2/area, one area per one section from each mouse, three mice) are shown. Gray and black bars indicated CB-MSCs transplanted and PBS-injected groups of mice, respectively (*p<0.05, Student's t-test).

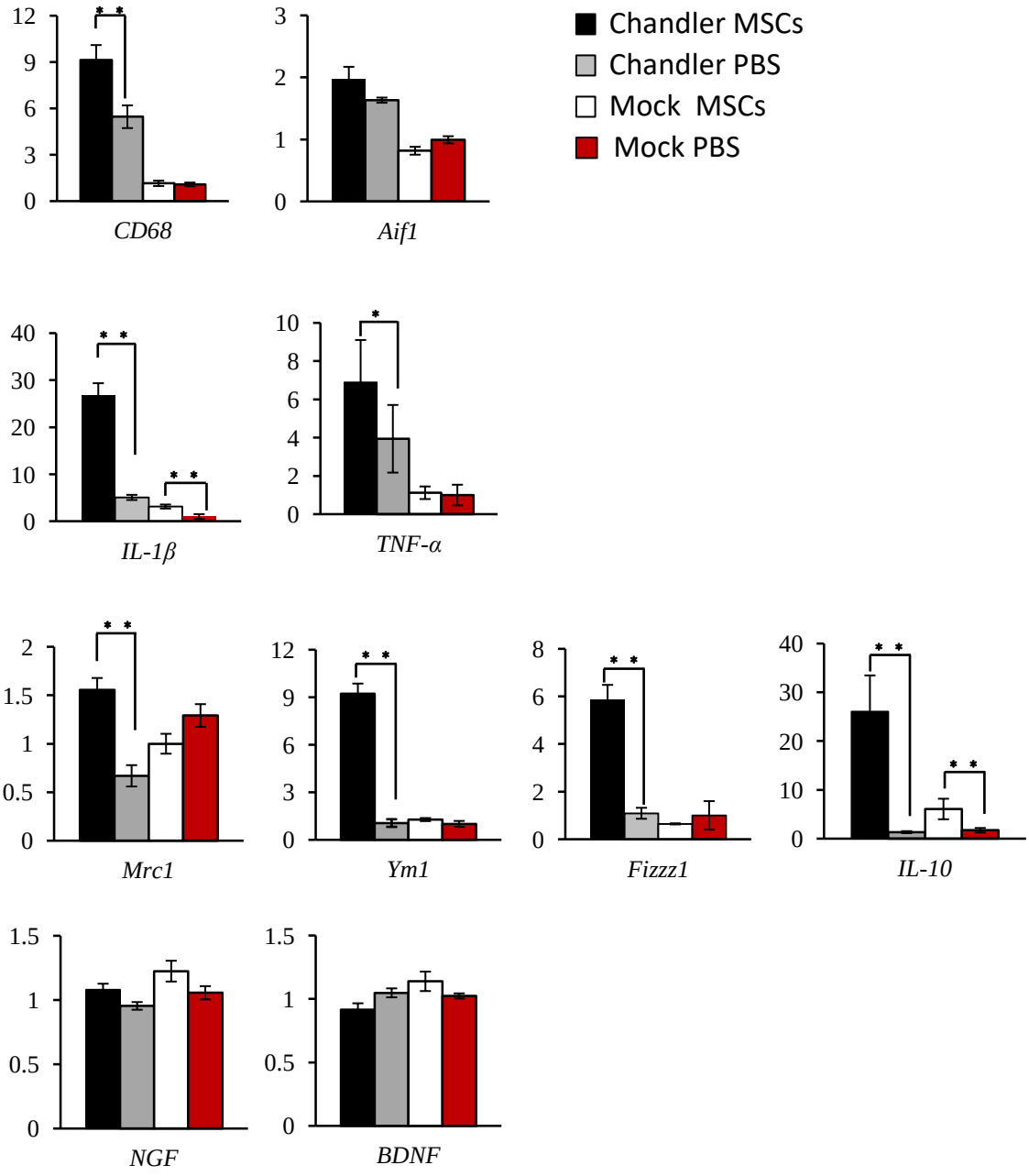

Fig II-6. Gene expression analysis.

CB-MSCs (1×10^5 cells in 2 μl PBS) were transplanted to the Chandler strain-infected mice (n = 3, black bars "Chandler MSCs") and mock-infected mice (n = 3, white bars "Mock MSCs") at 120 dpi. The same volume of PBS was injected to the Chandler strain-infected mice (n = 3, gray bars "Chandler PBS") and mock-infected mice (n = 3, red bars "Mock PBS") as a sham-operation group. At the 145 dpi, 21 days after transplantation, mice were sacrificed and hippocampus were collected for total RNA isolation. qRT- PCR was performed as described in Material and Methods. Gene expressions (Mean ± SD) of *CD68*, *Aif1* (Iba-1), *TNF-α, IL-1β, Mrc1*, *Ym1*, *Fizz1*,*IL-10, NGF and BDNF* in each group that are relative to mock-infected, sham-operated group are shown. Only the significant differences between CB-MSCs transplanted group and PBS injected group are shown. *, $p < 0.05$; **, $p < 0.01$, one-way ANOVA with Tukey *post hoc* tests.

prion-infected mice.

DISCUSSION

The primary purpose of this study is to analyze the efficacy of autologus MSCs transplantation on the treatment of prion diseases. Previously, my laboratory reported that transplantation of immortalized human MSCs prolonged the survival of mice infected with prions (Song *et al.*, 2009). That experiment was heterologous MSCs transplantation, where human PrP^{C} from human MSCs exists. It is well known that heterologous PrP^{C} interferes PrP^{Sc} formation of homologous PrP^{C} and PrP^{Sc} combination (Horiuchi *et al.*, 2000; Prusiner *et al.*, 1990). Thus one question arose was that the prolongation of survival may not be caused by any direct or indirect neuroprotective effect of human MSCs but just inhibition of PrP^{Sc} formation by human PrP^{C} produced by human MSCs. Another concern arose was that the use of immortalized MSCs caused an apparent protective effect due to a higher proliferation ability (Song *et al.*, 2009). However, I showed that autologous and un-immortalized MCSs transplantation prolonged the survival of mice infected with prions even when transplanted at 120 dpi, early clinical phase of the Chandler strain-infected mice. Kinetics of PrP^{Sc} accumulation revealed that no difference was observed in PrP^{Sc} level between MSCs-transplanted and sham operation group (Fig. II-4). This indicates that mouse CB-MSCs exert neuroprotective potential without inhibiting PrP^{Sc} formation.

In prion-infected mice, microglial activation is often associated spatially to the brain regions where PrP^{Sc} accumulates before the clinical onset (Sasaki *et al.*, 1993; Williams *et al.*, 1997; Williams *et al.*, 1994). However, it is controversial whether activated microglia exert

neuroprotective or neurotoxic function. Blockade of colony-stimulation factor receptor 1 signaling resulted in the prolongation of survival of prion-infected mice, accompanied with reduced microglial activation (Gomez-Nicola *et al.*, 2013). Vice versa, knockout of CD40 ligand shortened the survival of mice infected with prions with enhanced microglial activation (Burwinkel *et al.*, 2004). These facts suggest the detrimental effect of activated microglia in prion diseases. On the contrary, depletion of microglia from cerebellar slice culture resulted in the increase in PrP^{Sc} accumulation and consequently severe neuronal loss (Falsig *et al.*, 2008; Zhu *et al.*, 2016). My laboratory recently reported that prion-infected CD14-deficient mice showed prolonged survival with increased activation of microglia compared with wild-type mice (Sakai *et al.*, 2013). These reports suggest neuroprotective roles of microglia. In this study, prion-infected mice that were transplanted with CB-MSCs survived longer than mice in sham-operated group and showed increased microglial activation without reduction of PrP^{Sc} level (Figs. II-4 & II-5). The results suggest that the enhancement of microglia activation by CB-MSCs partly mitigated the disease progression without influencing the clearance of PrP^{Sc}. In the Alzhemier's disease (AD) model mice, microglial activation in the early stage of the disease is thought to be neuroprotective because of Aβ clearing functions by phagocytosis and by the production of Aβ-degrading enzyme (El Khoury *et al.*, 2007; Hickman *et al.*, 2008). However, phagocytic activity is attenuated by the stimulation of pro-inflammatory cytokine (Koenigsknecht-Talboo & Landreth, 2005). It is well-known that up-regulation of pro-inflammatory cytokines such as *IL-1β, TNFα, and IL-6 w*ith the disease progression in prion diseases (Campbell *et al.*, 1994; Hwang *et al.*, 2009; Kordek *et al.*, 1996). Here I showed further up-regulation of *IL-1β* gene expression in CB-MSCs transplanted prion-infected mice (Fig. II-6). Thus, it is conceivable that the microglia further activated by CB-MSCs transplantation have little effect on the clearance of PrP^{Sc}. The intracerebral injection of lipopolysaccharide induced microglial activation with marked production of

IL-1β but little clearance of PrP^{Sc} (Hughes *et al.*, 2010), supporting the result in this study.

Immunomodulation is believed to be one of the mechanism of neuroprotective effect of MSCs in neurodegenerative diseases and traumatic injuries. (Kyurkchiev *et al.*, 2014; Ohtaki *et al.*, 2008). The enhancement of microglial activation in CB-MSCs transplanted prion-infected mice appears immunomodulatory effect by CB-MSCs. Concurrent with the further microglial activation, expression of pro-inflammatory cytokine genes, *IL-1β* and *TNF-α*, was up-regulated more in CB-MSCs transplanted prion-infected mice than sham-operated prion-infected mice. Interestingly, gene expression of *IL-10*, anti-inflammatory cytokines that stimulates microglia to shift M2-type activation state, and gene expressions of *Ym1* and *Fizz1*, well-known M2-type microglia activation marker genes, were also up-regulated in CB-MSCs transplanted prion-infected mice (Fig. II-6). The result suggests that the CB-MSCs influence the microglial activation state and microglia polarized more to M2-type activation state. The enhancement of microglial activation in response to bone marrow-derived MSCs (BM-MSCs) transplantation with improvement of the cognitive decline was also reported in AD model mice (Lee *et al.*, 2010). In AD model mice, expression of *Ym1* and *Fizz1* genes and anti-inflammatory cytokine *IL-4* gene were up-regulated, suggesting the M2-type activation of microgila. Moreover, different from my result, expression of pro-inflammatory cytokines genes, *IL-1β* and *TNF-α*, was down-regulated. It is unknown whether difference of MSCs origin, *i.e.*, isolated from compact bone in the current study, while isolated from bone marrow in that study, or difference in pathobiology between prion diseases and AD attributed to the difference in pro-inflammatory cytokine gene expression. Interestingly, transplantation of BM-MSCs to rat model of traumatic brain injury reduced number of microglia accompanied with down-regulation of some of pro-inflammatory cytokine gene expressions but up-regulation of some of anti-inflammatory cytokine genes (Zhang *et al.*, 2013). This also suggests that microglia shift to M2-type

activation state in the presence of MSCs in response the acute traumatic injury. It is expected that neuro-pathobiology of acute traumatic injury and slow progressive encephalopathies such as AD and prion diseases differ each other; however, these findings suggests that MSCs could differently modulate microglial activation state to M2-type by responding each disease condition to exert neuroprotective functions. M2-type of microgila is reported to able to produce anti-inflammatory cytokines and neurotropic factors (Chio *et al.*, 2015), thus, it is possible that alternatively activated microglia facilitates neuroprotection and regeneration.

Other mechanisms of neuroprotection by MSCs includes protection of neurons or neural cells by producing neurotrophic factors such as BDNF and HGF (Bai *et al.*, 2012; Chopp & Li, 2002), neuronal differentiation or stimulation of differentiation of endogenous neural stem cells (Croft & Przyborski, 2009; Munoz *et al.*, 2005), or neurovascularization by producing VEGF (Toyama *et al.*, 2009), or decreasing oxidative stress (Calio *et al.*, 2014). Song *et al* reported that human BM-MSCs transplanted to prion-infected mice produced various neurotrophic factors such as NGF, BDNF, NT3/4 and VEGF (Song *et al*., 2009). In the current study, I used primary CB-MSCs without any genetic modification or labeling, in order to exclude any clonal or gene-modification effects. Thus, I could neither assess the production of growth factors by CB-MSCs nor assess the distribution and fate of transplanted CB-MSCs, which is also important information on considering the mechanism of neuroprotection by MSCs. Experiments are now on going to address these issues.

Here I showed that the autologous transplantation of CB-MSCs mitigated the disease progression of prion-infected mice. The CB-MSCs transplantation did not influence prion PrP^{Sc} accumulation but enhanced microglial activation that appeared to be polarized to M2-type activation state. It remains to be elucidated whether M2-type polarized microglia exert neuroprotective roles against prion propagation. However, the results in this study accelerate further studies for applying regenerative medicine to the treatment of prion

diseases.

BRIEF SUMMARY

Prion diseases are fatal neurodegenerative disorders of humans and animals and no effective treatments are available to date. Previous studies in my laboratory showed that human mesenchymal stem cells (MSCs) migrated to brain lesions and prolonged the survival of mice infected with prions. However, autologous transplantation is an appropriate model for the evaluation of the effect of MSCs on prion diseases. Therefore, I isolated and purified MSCs from mice femur and tibia (compact bone-derived MSCs, CB-MSCs). Flow cytometric analysis showed that CB-MSCs were negative for myeloid stem cell-derived cell markers CD11b and CD45, but positive for a couple of markers, such as Sca-1, CD105, and CD90.2, which were reported to be expressed on MSCs. Then I confirmed migration ability of CB-MSCs to brain extracts from the Chandler strain-infected mice using in vitro migration assay. Intra-hippocampus transplantation of CB-MSCs at 120 days post inoculation marginally but significantly prolonged survival of mice infected with the Chandler prion strain. The CB-MSCs transplantation did not influence the accumulation of disease-specific prion protein (PrP^{Sc}); however, the CB-MSCs transplantation enhanced microglial activation that appeared to be polarized to M2-type activation state. These results suggest that autologous MSC transplantation is possible treatment for prion diseases and that modification of microglial activation may be a target for therapeutics of neurodegenerative diseases.

CONCLUSION

A number of compounds have been reported to inhibit PrP^{Sc} formation; however the therapeutic effects are limited and further efforts on exploring therapeutic compounds are required. Immortalized cells that permit prion propagation, such as neuroblastoma cells, have been used for the screening of anti-prion compounds. However, one of the technical limitations in using cells persistently infected with prions for screening of anti-prion compounds is the requirement for PK treatment to remove PrP^{C} from the cells. It is well known that PrP^{Sc} comprises PK-sensitive PrP^{Sc} (PrP^{Sc}-sen) and PK-resistant PrP^{Sc} (PrP^{Sc}-res), and that PrP^{Sc}-sen is reported to possess higher infectivity and conversion activity than PrP^{Sc}-res. PK treatment digests PrP^{Sc}-sen so that the effect of compounds on PrP^{Sc} formation may be overlooked. Therefore, in the Chapter I, I established a novel cell-based ELISA in which PrP^{Sc} can be directly detected from prion-infected cells using anti-PrP monoclonal antibody (mAb 132) without PK treatment. MAb 132 could detect both PrP^{Sc}-sen and PrP^{Sc}-res even if all PrP^{Sc} molecules were not detected. The analytical dynamic range for PrP^{Sc} detection was approximately 1 log. The coefficient of variation and signal-to-background ratio were 7–11% and 2.5–3.3, respectively, demonstrating the reproducibility of this assay. The addition of a cytotoxicity assay immediately before PrP^{Sc} detection did not affect the following PrP^{Sc} detection. Thus, all the procedures including cell culture, cytotoxicity assay, and PrP^{Sc} detection were completed in the same plate. The simplicity and non-requirement for cell lysis or PK treatment are advantages for the high throughput screening of anti-prion compounds.

Another direction for the therapeutics of prion disease is the protection of neurodegeneration. The autologous mesenchymal stem cells (MSCs) transplantation has been reported to show tendency of functional recovery or partial improvement in patients of stroke in neurodegenerative disorders such as stroke and spinal cord injury. In prion diseases, it is reported that allogenic transplantation of human MSCs mitigated the disease progression in prion-infected mice. However, autologous MSCs transplantation is required for the practical application for the patients. Thus, in the Chapter II, I evaluated the efficacy of mouse MSCs transplantation into prion-infected mice. Plastic adherent cells isolated from compact bone of mice were further purified by elimination of CD11b- and CD45-positive cells and used as compact bone-derived MSCs (CB-MSCs). Flow cytometric analysis showed that CB-MSCs were negative for CD11b and CD45, but positive for a serious of markers that were reported to be expressed on MSCs. Intra-hippocampus transplantation of CB-MSCs at 120 days post inoculation marginally but significantly prolonged survival of mice infected with the Chandler prion strain. The CB-MSCs transplantation did not influence the accumulation of PrP^{Sc}-res; however, the CB-MSCs transplantation enhanced microglial activation that appeared to be polarized to M2-type activation state. These results suggest that the autologous MSC transplantation is possible treatment for prion diseases and that modification of microglial activation may be a target for therapeutics of neurodegenerative diseases.

In this thesis, I established the novel cell-based ELISA that will be useful for the screening of anti-prion compounds. Since the mechanism of PrP^{Sc} detection differs from other screening methods used thus far, it should have potential for finding new therapeutic compounds. I also showed that the autologous transplantation of MSCs prolonged the survival of mice infected with prions. The results open the possibility of regenerative medicine for the

prion disease. I believe that the results described in this thesis will accelerate further researches on the establishment of therapeutics for prion diseases.

ACKNOWLEDGEMENTS

My deepest gratitude to my supervisor, Professor Motohiro Horiuchi (Laboratory of Veterinary Hygiene, Department of Applied Veterinary Sciences, Graduate School of Veterinary Medicine, Hokkaido University) for his constant encouragement and patient discussions throughout my study life and the preparation of the manuscript. He offered me the valuable chance as a foreign Ph. D student to study in his laboratory and generous guided me in both research and life.

I also would like to express my appreciation to Dr. Rie Hasebe and Dr. Takeshi Yamasaki (Laboratory of Veterinary Hygiene, Department of Applied Veterinary Sciences, Graduate School of Veterinary Medicine, Hokkaido University) who always support me to understand my research well with helpful discussions and warm encouragement.

I am also greatly indebted to the major advisory supervisors, Professor Katsumi Doh-ura (Department of Neurochemistry, Tohoku University Graduate School of Medicine), Professor Hirofumi Sawa (Division of Molecular Pathobiology, Research Center for Zoonosis Control, Hokkaido University) and Associate Professor Atsushi Kobayashi (Laboratory of Comparative Pathology, Graduate School of Veterinary Medicine, Hokkaido University) for valuable and helpful discussions throughout my Ph. D course.

I deeply grateful to Mr. Akio Suzuki, Mr. Ryo Hayashi, Dr. Minori Kuroda, and Dr. Yuji Hirai for the teaching of new experiment technique in my study, and thank to all the members of Laboratory of Veterinary Hygiene for their supports and warm encouragement.

Last my thanks would go to my beloved family and friends for their loving considerations and great encouragement. I also owe my sincere gratitude to China Scholarship Council and Leading program in Hokkaido University for the supporting of my study and life in Japan.

REFERENCES

Aguzzi, A., Baumann, F. & Bremer, J. (2008). The prion's elusive reason for being. *Annu Rev Neurosci,* **31**, 439-477.

Azizi, S. A., Stokes, D., Augelli, B. J., DiGirolamo, C. & Prockop, D. J. (1998). Engraftment and migration of human bone marrow stromal cells implanted in the brains of albino rats--similarities to astrocyte grafts. *Proc Natl Acad Sci USA,* **95**, 3908-3913.

Bai, L., Lennon, D. P., Caplan, A. I., DeChant, A., Hecker, J., Kranso, J., Zaremba, A. & Miller, R. H. (2012). Hepatocyte growth factor mediates mesenchymal stem cell-induced recovery in multiple sclerosis models. *Nat Neurosci,* **15**, 862-870.

Blandini, F., Cova, L., Armentero, M. T., Zennaro, E., Levandis, G., Bossolasco, P., Calzarossa, C., Mellone, M., Giuseppe, B., Deliliers, G. L., Polli, E., Nappi, G. & Silani, V. (2010). Transplantation of undifferentiated human mesenchymal stem cells protects against 6-hydroxydopamine neurotoxicity in the rat. *Cell Transplant,* **19**, 203-217.

Boucherie, C., Schafer, S., Lavand'homme, P., Maloteaux, J. M. & Hermans, E. (2009). Chimerization of astroglial population in the lumbar spinal cord after mesenchymal stem cell transplantation prolongs survival in a rat model of amyotrophic lateral sclerosis. *J Neurosci Res,* **87**, 2034-2046.

Brandner, S., Raeber, A., Sailer, A., Blattler, T., Fischer, M., Weissmann, C. & Aguzzi, A. (1996). Normal host prion protein (PrP^{C}) is required for scrapie spread within the

central nervous system. *Proc Natl Acad Sci USA,* **93**, 13148-13151.

Bremer, J., Baumann, F., Tiberi, C., Wessig, C., Fischer, H., Schwarz, P., Steele, A. D., Toyka, K. V., Nave, K. A., Weis, J. & Aguzzi, A. (2010). Axonal prion protein is required for peripheral myelin maintenance. *Nat Neurosci,* **13**, 310-318.

Brown, D. R., Qin, K., Herms, J. W., Madlung, A., Manson, J., Strome, R., Fraser, P. E., Kruck, T., von Bohlen, A., Schulz-Schaeffer, W., Giese, A., Westaway, D. & Kretzschmar, H. (1997). The cellular prion protein binds copper in vivo. *Nature,* **390**, 684-687.

Bueler, H., Aguzzi, A., Sailer, A., Greiner, R. A., Autenried, P., Aguet, M. & Weissmann, C. (1993). Mice devoid of PrP are resistant to scrapie. *Cell,* **73**, 1339-1347.

Bueler, H., Fischer, M., Lang, Y., Bluethmann, H., Lipp, H. P., DeArmond, S. J., Prusiner, S. B., Aguet, M. & Weissmann, C. (1992). Normal development and behaviour of mice lacking the neuronal cell-surface PrP protein. *Nature,* **356**, 577-582.

Burwinkel, M., Schwarz, A., Riemer, C., Schultz, J., van Landeghem, F. & Baier, M. (2004). Rapid disease development in scrapie-infected mice deficient for CD40 ligand. *EMBO Rep,* **5**, 527-531.

Calio, M. L., Marinho, D. S., Ko, G. M., Ribeiro, R. R., Carbonel, A. F., Oyama, L. M., Ormanji, M., Guirao, T. P., Calio, P. L., Reis, L. A., Simoes Mde, J., Lisboa-Nascimento, T., Ferreira, A. T. & Bertoncini, C. R. (2014). Transplantation of bone marrow mesenchymal stem cells decreases oxidative stress, apoptosis, and hippocampal damage in brain of a spontaneous stroke model. *Free Radic Biol Med,* **70**, 141-154.

Campbell, I. L., Eddleston, M., Kemper, P., Oldstone, M. B. & Hobbs, M. V. (1994).

Activation of cerebral cytokine gene expression and its correlation with onset of reactive astrocyte and acute-phase response gene expression in scrapie. *J Virol,* **68**, 2383-2387.

Caughey, B. & Raymond, G. J. (1991). The scrapie-associated form of PrP is made from a cell surface precursor that is both protease- and phospholipase-sensitive. *J Biol Chem,* **266**, 18217-18223.

Caughey, B. & Raymond, G. J. (1993). Sulfated polyanion inhibition of scrapie-associated PrP accumulation in cultured cells. *J Virol*, **67**, 643-650.

Chambers, S. M., Fasano, C. A., Papapetrou, E. P., Tomishima, M., Sadelain, M. & Studer, L. (2009). Highly efficient neural conversion of human ES and iPS cells by dual inhibition of SMAD signaling. *Nat Biotechnol,* **27**, 275-280.

Chao, Y. X., He, B. P. & Tay, S. S. (2009). Mesenchymal stem cell transplantation attenuates blood brain barrier damage and neuroinflammation and protects dopaminergic neurons against MPTP toxicity in the substantia nigra in a model of Parkinson's disease. *J Neuroimmunol,* **216**, 39-50.

Chen, J., Li, Y., Wang, L., Lu, M., Zhang, X. & Chopp, M. (2001). Therapeutic benefit of intracerebral transplantation of bone marrow stromal cells after cerebral ischemia in rats. *J Neurol Sci,* **189**, 49-57.

Chesebro, B., Trifilo, M., Race, R., Meade-White, K., Teng, C., LaCasse, R., Raymond, L., Favara, C., Baron, G., Priola, S., Caughey, B., Masliah, E. & Oldstone, M. (2005). Anchorless prion protein results in infectious amyloid disease without clinical scrapie. *Science*, 308, 1435-1439.

Chio, C. C., Lin, M. T. & Chang, C. P. (2015). Microglial activation as a compelling target

for treating acute traumatic brain injury. *Curr Med Chem*, 22, 759-770.

Chopp, M. & Li, Y. (2002). Treatment of neural injury with marrow stromal cells. *Lancet Neurol*, **1**, 92-100.

Collinge, J., Whittington, M. A., Sidle, K. C., Smith, C. J., Palmer, M. S., Clarke, A. R. & Jefferys, J. G. (1994). Prion protein is necessary for normal synaptic function. *Nature*, **370**, 295-297.

Croft, A. P. & Przyborski, S. A. (2009). Mesenchymal stem cells expressing neural antigens instruct a neurogenic cell fate on neural stem cells. *Exp Neurol*, **216**, 329-341.

Cronier, S., Gros, N., Tattum, M. H., Jackson, G. S., Clarke, A. R., Collinge, J. & Wadsworth, J. D. (2008). Detection and characterization of proteinase K-sensitive disease-related prion protein with thermolysin. *Biochem J*, **416**, 297-305.

Dimos, J. T., Rodolfa, K. T., Niakan, K. K., Weisenthal, L. M., Mitsumoto, H., Chung, W., Croft, G. F., Saphier, G., Leibel, R., Goland, R., Wichterle, H., Henderson, C. E. & Eggan, K. (2008). Induced pluripotent stem cells generated from patients with ALS can be differentiated into motor neurons. *Science*, **321**, 1218-1221.

Dominici, M., Le Blanc, K., Mueller, I., Slaper-Cortenbach, I., Marini, F., Krause, D., Deans, R., Keating, A., Prockop, D. & Horwitz, E. (2006). Minimal criteria for defining multipotent mesenchymal stromal cells. The International Society for Cellular Therapy position statement. *Cytotherapy*, **8**, 315-317.

El Khoury, J., Toft, M., Hickman, S. E., Means, T. K., Terada, K., Geula, C. & Luster, A. D. (2007). Ccr2 deficiency impairs microglial accumulation and accelerates progression of Alzheimer-like disease. *Nat Med*, **13**, 432-438.

Falsig, J., Julius, C., Margalith, I., Schwarz, P., Heppner, F. L. & Aguzzi, A. (2008). A

versatile prion replication assay in organotypic brain slices. *Nat Neurosci,* **11**, 109-117.

Ferreira, N. C., Marques, I. A., Conceicao, W. A., Macedo, B., Machado, C. S., Mascarello, A., Chiaradia-Delatorre, L. D., Yunes, R. A., Nunes, R. J., Hughson, A. G., Raymond, L. D., Pascutti, P. G., Caughey, B. & Cordeiro, Y. (2014). Anti-prion activity of a panel of aromatic chemical compounds: in vitro and in silico approaches. *PloS One,* **9**, e84531.

Friedrich, M. A., Martins, M. P., Araujo, M. D., Klamt, C., Vedolin, L., Garicochea, B., Raupp, E. F., Sartori El Ammar, J., Machado, D. C., Costa, J. C., Nogueira, R. G., Intra-arterial infusion of autologous bone marrow mononuclear cells in patients with moderate to severe middle cerebral artery acute ischemic stroke. *Cell Transplant,* **21 Suppl 1**, S13-21.

Furuoka, H., Yabuzoe, A., Horiuchi, M., Tagawa, Y., Yokoyama, T., Yamakawa, Y., Shinagawa, M. & Sata, T. (2005). Effective antigen-retrieval method for immunohistochemical detection of abnormal isoform of prion proteins in animals. *Acta Neuropathol,* **109**, 263-271.

Ghaemmaghami, S., May, B. C., Renslo, A. R. & Prusiner, S. B. (2010). Discovery of 2-aminothiazoles as potent antiprion compounds. *J Virol*, **84**, 3408-3412.

Godsave, S. F., Wille, H., Kujala, P., Latawiec, D., DeArmond, S. J., Serban, A., Prusiner, S. B. & Peters, P. J. (2008). Cryo-immunogold electron microscopy for prions: toward identification of a conversion site. *J Neurosci*, **28**, 12489-12499.

Gomez-Nicola, D., Fransen, N. L., Suzzi, S. & Perry, V. H. (2013). Regulation of microglial proliferation during chronic neurodegeneration. *J Neurosci,* **33**, 2481-2493.

Goold, R., Rabbanian, S., Sutton, L., Andre, R., Arora, P., Moonga, J., Clarke, A. R.,

Schiavo, G., Jat, P., Collinge, J. & Tabrizi, S. J. (2011). Rapid cell-surface prion protein conversion revealed using a novel cell system. *Nat Commun*, **2**, 281.

Heal, W., Thompson, M. J., Mutter, R., Cope, H., Louth, J. C. & Chen, B. (2007). Library synthesis and screening: 2,4-diphenylthiazoles and 2,4-diphenyloxazoles as potential novel prion disease therapeutics. *J Med Chem*, **50**, 1347-1353.

Hellmann, M. A., Panet, H., Barhum, Y., Melamed, E. & Offen, D. (2006). Increased survival and migration of engrafted mesenchymal bone marrow stem cells in 6-hydroxydopamine-lesioned rodents. *Neurosci Lett*, **395**, 124-128.

Hickman, S. E., Allison, E. K. & El Khoury, J. (2008). Microglial dysfunction and defective beta-amyloid clearance pathways in aging Alzheimer's disease mice. *J Neurosci*, **28**, 8354-8360.

Hofstetter, C. P., Schwarz, E. J., Hess, D., Widenfalk, J., El Manira, A., Prockop, D. J. & Olson, L. (2002). Marrow stromal cells form guiding strands in the injured spinal cord and promote recovery. *Proc Natl Acad Sci USA*, **99**, 2199-2204.

Honmou, O., Houkin, K., Matsunaga, T., Niitsu, Y., Ishiai, S., Onodera, R., Waxman, S. G. & Kocsis, J. D. (2011). Intravenous administration of auto serum-expanded autologous mesenchymal stem cells in stroke. *Brain*, **134**, 1790-1807.

Horiuchi, M., Mochizuki, M., Ishiguro, N., Nagasawa, H. & Shinagawa, M. (1997). Epitope mapping of a monoclonal antibody specific to feline panleukopenia virus and mink enteritis virus. *J Vet Med Sci*, **59**, 133-136.

Horiuchi, M., Priola, S. A., Chabry, J. & Caughey, B. (2000). Interactions between heterologous forms of prion protein: binding, inhibition of conversion, and species barriers. *Proc Natl Acad Sci USA*, **97**, 5836-5841.

Hosokawa-Muto, J., Kamatari, Y. O., Nakamura, H. K. & Kuwata, K. (2009). Variety of antiprion compounds discovered through an in silico screen based on cellular-form prion protein structure: Correlation between antiprion activity and binding affinity. *Antimicrob Agents Chemother*, **53**, 765-771.

Hughes, M. M., Field, R. H., Perry, V. H., Murray, C. L. & Cunningham, C. (2010). Microglia in the degenerating brain are capable of phagocytosis of beads and of apoptotic cells, but do not efficiently remove PrP^{Sc}, even upon LPS stimulation. *Glia*, **58**, 2017-2030.

Hwang, D., Lee, I. Y., Yoo, H., Gehlenborg, N., Cho, J. H., Petritis, B., Baxter, D., Pitstick, R., Young, R., Spicer, D., Price, N. D., Hohmann, J. G., Dearmond, S. J., Carlson, G. A. & Hood, L. E. (2009). A systems approach to prion disease. *Mol Syst Biol*, **5**, 252.

Ishiguro, N., Inoshima, Y., Sassa, Y. & Takahashi, T. (2009). Molecular characterization of chicken prion proteins by C-terminal-specific monoclonal antibodies. *Vet Immunol Immunopathol*, **128**, 402-406.

Karapetyan, Y. E., Sferrazza, G. F., Zhou, M., Ottenberg, G., Spicer, T., Chase, P., Fallahi, M., Hodder, P., Weissmann, C. & Lasmezas, C. I. (2013). Unique drug screening approach for prion diseases identifies tacrolimus and astemizole as antiprion agents. *Proc Natl Acad Sci USA*, **110**, 7044-7049.

Karussis, D., Karageorgiou, C., Vaknin-Dembinsky, A., Gowda-Kurkalli, B., Gomori, J. M., Kassis, I., Bulte, J. W., Petrou, P., Ben-Hur, T., Abramsky, O. & Slavin, S. (2010). Safety and immunological effects of mesenchymal stem cell transplantation in patients with multiple sclerosis and amyotrophic lateral sclerosis. *Arch Neurol*, **67**,

1187-1194.

Kim, C. L., Karino, A., Ishiguro, N., Shinagawa, M., Sato, M. & Horiuchi, M. (2004a). Cell-surface retention of PrPC by anti-PrP antibody prevents protease-resistant PrP formation. *J Gen Virol*, **85**, 3473-3482.

Kim, C. L., Umetani, A., Matsui, T., Ishiguro, N., Shinagawa, M. & Horiuchi, M. (2004b). Antigenic characterization of an abnormal isoform of prion protein using a new diverse panel of monoclonal antibodies. *Virology*, **320**, 40-51.

Kim, S., Chang, K. A., Kim, J., Park, H. G., Ra, J. C., Kim, H. S. & Suh, Y. H. (2012). The preventive and therapeutic effects of intravenous human adipose-derived stem cells in Alzheimer's disease mice. *PloS One*, **7**, e45757.

Kim, T. E., Kim, C. G., Kim, J. S., Jin, S., Yoon, S., Bae, H. R., Kim, J. H., Jeong, Y. H. & Kwak, J. Y. (2016). Three-dimensional culture and interaction of cancer cells and dendritic cells in an electrospun nano-submicron hybrid fibrous scaffold. *Int Nanomedicine*, **11**, 823-835.

Klamt, F., Dal-Pizzol, F., Conte da Frota, M. L., Jr., Walz, R., Andrades, M. E., da Silva, E. G., Brentani, R. R., Izquierdo, I. & Fonseca Moreira, J. C. (2001). Imbalance of antioxidant defense in mice lacking cellular prion protein. *Free radical biology & medicine* **30**, 1137-1144.

Klingenstein, R., Lober, S., Kujala, P., Godsave, S., Leliveld, S. R., Gmeiner, P., Peters, P. J. & Korth, C. (2006). Tricyclic antidepressants, quinacrine and a novel, synthetic chimera thereof clear prions by destabilizing detergent-resistant membrane compartments. *J Neurochem*, **98**, 748-759.

Kocisko, D. A., Baron, G. S., Rubenstein, R., Chen, J., Kuizon, S. & Caughey, B. (2003).

New inhibitors of scrapie-associated prion protein formation in a library of 2000 drugs and natural products. *J Virol*, **77**, 10288-10294.

Koenigsknecht-Talboo, J. & Landreth, G. E. (2005). Microglial phagocytosis induced by fibrillar beta-amyloid and IgGs are differentially regulated by proinflammatory cytokines. *J Neurosci*, **25**, 8240-8249.

Kordek, R., Nerurkar, V. R., Liberski, P. P., Isaacson, S., Yanagihara, R. & Gajdusek, D. C. (1996). Heightened expression of tumor necrosis factor alpha, interleukin 1 alpha, and glial fibrillary acidic protein in experimental Creutzfeldt-Jakob disease in mice. *Proc Natl Acad Sci USA*, **93**, 9754-9758.

Kuffer, A., Lakkaraju, A. K., Mogha, A., Petersen, S. C., Airich, K., Doucerain, C., Marpakwar, R., Bakirci, P., Senatore, A., Monnard, A., Schiavi, C., Nuvolone, M., Grosshans, B., Hornemann, S., Bassilana, F., Monk, K. R. & Aguzzi, A. (2016). The prion protein is an agonistic ligand of the G protein-coupled receptor Adgrg6. *Nature*, **536**, 464-468.

Kuroda, Y., Kitada, M., Wakao, S. & Dezawa, M. (2011). Bone marrow mesenchymal cells: how do they contribute to tissue repair and are they really stem cells *Arch Immunol Ther Exp*, **59**, 369-378.

Kuwata, K., Nishida, N., Matsumoto, T., Kamatari, Y. O., Hosokawa-Muto, J., Kodama, K., Nakamura, H. K., Kimura, K., Kawasaki, M., Takakura, Y., Shirabe, S., Takata, J., Kataoka, Y. & Katamine, S. (2007). Hot spots in prion protein for pathogenic conversion. *Proc Natl Acad Sci USA*, **104**, 11921-11926.

Kyurkchiev, D., Bochev, I., Ivanova-Todorova, E., Mourdjeva, M., Oreshkova, T., Belemezova, K. & Kyurkchiev, S. (2014). Secretion of immunoregulatory cytokines

by mesenchymal stem cells. *World J Stem Cells,* **6**, 552-570.

Lee, J. K., Jin, H. K., Endo, S., Schuchman, E. H., Carter, J. E. & Bae, J. S. (2010). Intracerebral transplantation of bone marrow-derived mesenchymal stem cells reduces amyloid-beta deposition and rescues memory deficits in Alzheimer's disease mice by modulation of immune responses. *StemCells,* **28**, 329-343.

Leidel, F., Eiden, M., Geissen, M., Kretzschmar, H. A., Giese, A., Hirschberger, T., Tavan, P., Schatzl, H. M. & Groschup, M. H. (2011). Diphenylpyrazole-derived compounds increase survival time of mice after prion infection. *Antimicrob Agents Chemother,* **55**, 4774-4781.

Li, Y., Chen, J., Zhang, C. L., Wang, L., Lu, D., Katakowski, M., Gao, Q., Shen, L. H., Zhang, J., Lu, M. & Chopp, M. (2005). Gliosis and brain remodeling after treatment of stroke in rats with marrow stromal cells. *Glia,* **49**, 407-417.

Mallucci, G., Dickinson, A., Linehan, J., Klohn, P. C., Brandner, S. & Collinge, J. (2003). Depleting neuronal PrP in prion infection prevents disease and reverses spongiosis. *Science,* **302**, 871-874.

Mallucci, G. R., Ratte, S., Asante, E. A., Linehan, J., Gowland, I., Jefferys, J. G. & Collinge, J. (2002). Post-natal knockout of prion protein alters hippocampal CA1 properties, but does not result in neurodegeneration. *EMBO J,* **21**, 202-210.

Marijanovic, Z., Caputo, A., Campana, V. & Zurzolo, C. (2009). Identification of an intracellular site of prion conversion. *PLoS Pathog*, **5**, e1000426.

Morikawa, S., Mabuchi, Y., Kubota, Y., Nagai, Y., Niibe, K., Hiratsu, E., Suzuki, S., Miyauchi-Hara, C., Nagoshi, N., Sunabori, T., Shimmura, S., Miyawaki, A., Nakagawa, T., Suda, T., Okano, H. & Matsuzaki, Y. (2009). Prospective

identification, isolation, and systemic transplantation of multipotent mesenchymal stem cells in murine bone marrow. *J Exp Med,* **206**, 2483-2496.

Munoz, J. R., Stoutenger, B. R., Robinson, A. P., Spees, J. L. & Prockop, D. J. (2005). Human stem/progenitor cells from bone marrow promote neurogenesis of endogenous neural stem cells in the hippocampus of mice. *Proc Natl Acad Sci USA,* **102**, 18171-18176.

Nakamitsu, S., Kurokawa, A., Yamasaki, T., Uryu, M., Hasebe, R. & Horiuchi, M. (2010). Cell density-dependent increase in the level of protease-resistant prion protein in prion-infected Neuro2a mouse neuroblastoma cells. *J Gen Virol,* **91**, 563-569.

Nakamura, K., Ito, Y., Kawano, Y., Kurozumi, K., Kobune, M., Tsuda, H., Bizen, A., Honmou, O., Niitsu, Y. & Hamada, H. (2004). Antitumor effect of genetically engineered mesenchymal stem cells in a rat glioma model. *Gene Ther,* **11**, 1155-1164.

Nombela-Arrieta, C., Ritz, J. & Silberstein, L. E. (2011). The elusive nature and function of mesenchymal stem cells. *Nat Rev Mol Cell Biol,* **12**, 126-131.

Ohsawa, N., Song, C. H., Suzuki, A., Furuoka, H., Hasebe, R. & Horiuchi, M. (2013). Therapeutic effect of peripheral administration of an anti-prion protein antibody on mice infected with prions. *Microbiol Immunol,* **57**, 288-297.

Ohtaki, H., Ylostalo, J. H., Foraker, J. E., Robinson, A. P., Reger, R. L., Shioda, S. & Prockop, D. J. (2008). Stem/progenitor cells from bone marrow decrease neuronal death in global ischemia by modulation of inflammatory/immune responses. *Proc Natl Acad Sci USA,* **105**, 14638-14643.

Park, H. J., Shin, J. Y., Lee, B. R., Kim, H. O. & Lee, P. H. (2012). Mesenchymal stem cells augment neurogenesis in the subventricular zone and enhance differentiation of

neural precursor cells into dopaminergic neurons in the substantia nigra of a parkinsonian model. *Cell Transplant*, **21**, 1629-1640.

Pastrana, M. A., Sajnani, G., Onisko, B., Castilla, J., Morales, R., Soto, C. & Requena, J. R. (2006). Isolation and characterization of a proteinase K-sensitive PrPSc fraction. *Biochemistry,* **45**, 15710-15717.

Pittenger, M. F., Mackay, A. M., Beck, S. C., Jaiswal, R. K., Douglas, R., Mosca, J. D., Moorman, M. A., Simonetti, D. W., Craig, S. & Marshak, D. R. (1999). Multilineage potential of adult human mesenchymal stem cells. *Science,* **284**, 143-147.

Priola, S. A. & Caughey, B. (1994). Inhibition of scrapie-associated PrP accumulation. Probing the role of glycosaminoglycans in amyloidogenesis. *Mol Neurobiol,* **8**, 113-120.

Prusiner, S. B. (1994). Biology and genetics of prion diseases. *Annu Rev Microbiol,* **48**, 655-686.

Prusiner, S. B. (1998). Prions. *Proc Natl Acad Sci USA* **95**, 13363-13383.

Prusiner, S. B., Scott, M., Foster, D., Pan, K. M., Groth, D., Mirenda, C., Torchia, M., Yang, S. L., Serban, D., Carlson, G. A. & et al. (1990). Transgenetic studies implicate interactions between homologous PrP isoforms in scrapie prion replication. *Cell*, **63**, 673-686.

Qayyum, A. A., Haack-Sorensen, M., Mathiasen, A. B., Jorgensen, E., Ekblond, A. & Kastrup, J. (2012). Adipose-derived mesenchymal stromal cells for chronic myocardial ischemia (MyStromalCell Trial): study design. *Regen Med*, **7**, 421-428.

Qi, Y., Feng, G. & Yan, W. (2012). Mesenchymal stem cell-based treatment for cartilage defects in osteoarthritis. *Mol Biol Rep* **39**, 5683-5689*Biochemistry*, **45**, 15710-15717.

Radovanovic, I., Braun, N., Giger, O. T., Mertz, K., Miele, G., Prinz, M., Navarro, B. & Aguzzi, A. (2005). Truncated prion protein and Doppel are myelinotoxic in the absence of oligodendrocytic PrP^{C}. *J Neurosci*, **25**, 4879-4888.

Relano-Gines, A., Lehmann, S., Bencsik, A., Herva, M. E., Torres, J. M. & Crozet, C. A. (2011). Stem cell therapy extends incubation and survival time in prion-infected mice in a time window-dependant manner. *J Infect Dis*, **204**, 1038-1045.

Ren, G., Zhao, X., Zhang, L., Zhang, J., L'Huillier, A., Ling, W., Roberts, A. I., Le, A. D., Shi, S., Shao, C. & Shi, Y. (2010). Inflammatory cytokine-induced intercellular adhesion molecule-1 and vascular cell adhesion molecule-1 in mesenchymal stem cells are critical for immunosuppression. *J Immunol*, **184**, 2321-2328.

Rosado-de-Castro, P. H., Mendez-Otero, R. & Freitas, G. R. (2012). Intra-arterial infusion of autologous bone marrow mononuclear cells in patients with moderate to severe middle cerebral artery acute ischemic stroke. *Cell Transplant*, **21 Suppl 1**, S13-21.

Rouvinski, A., Karniely, S., Kounin, M., Moussa, S., Goldberg, M. D., Warburg, G., Lyakhovetsky, R., Papy-Garcia, D., Kutzsche, J., Korth, C., Carlson, G. A., Godsave, S. F., Peters, P. J., Luhr, K., Kristensson, K. & Taraboulos, A. (2014). Live imaging of prions reveals nascent PrP^{Sc} in cell-surface, raft-associated amyloid strings and webs. *J Cell Biol*, **204**, 423-441.e271-276.

Safar, J., Wille, H., Itri, V., Groth, D., Serban, H., Torchia, M., Cohen, F. E. & Prusiner, S. B. (1998). Eight prion strains have PrP(Sc) molecules with different conformations. *Nat Med*, **4**, 1157-1165.

Safar, J. G., Geschwind, M. D., Deering, C., Didorenko, S., Sattavat, M., Sanchez, H., Serban, A., Vey, M., Baron, H., Giles, K., Miller, B. L., Dearmond, S. J. &

Prusiner, S. B. (2005). Diagnosis of human prion disease. *Proc Natl Acad Sci USA,* **102**, 3501-3506.

Sakai, K., Hasebe, R., Takahashi, Y., Song, C. H., Suzuki, A., Yamasaki, T. & Horiuchi, M. (2013). Absence of CD14 delays progression of prion diseases accompanied by increased microglial activation. *J Virol,* **87**, 13433-13445.

Sasaki, A., Hirato, J. & Nakazato, Y. (1993). Immunohistochemical study of microglia in the Creutzfeldt-Jakob diseased brain. *Acta Neuropathol,* **86**, 337-344.

Schatzl, H. M., Laszlo, L., Holtzman, D. M., Tatzelt, J., DeArmond, S. J., Weiner, R. I., Mobley, W. C. & Prusiner, S. B. (1997). A hypothalamic neuronal cell line persistently infected with scrapie prions exhibits apoptosis. *J Virol,* **71**, 8821-8831.

Silber, B. M., Gever, J. R., Rao, S., Li, Z., Renslo, A. R., Widjaja, K., Wong, C., Giles, K., Freyman, Y., Elepano, M., Irwin, J. J., Jacobson, M. P. & Prusiner, S. B. (2014). Novel compounds lowering the cellular isoform of the human prion protein in cultured human cells. *Bioorg Med Chem,* **22**, 1960-1972.

Silveira, J. R., Raymond, G. J., Hughson, A. G., Race, R. E., Sim, V. L., Hayes, S. F. & Caughey, B. (2005). The most infectious prion protein particles. *Nature,* **437**, 257-261.

Snykers, S., De Kock, J., Rogiers, V. & Vanhaecke, T. (2009). In vitro differentiation of embryonic and adult stem cells into hepatocytes: state of the art. *Stem cells,* **27**, 577-605.

Song, C. H., Furuoka, H., Kim, C. L., Ogino, M., Suzuki, A., Hasebe, R. & Horiuchi, M. (2008). Effect of intraventricular infusion of anti-prion protein monoclonal antibodies on disease progression in prion-infected mice. *J Gen Virol,* **89**, 1533-1544.

Song, C. H., Honmou, O., Furuoka, H. & Horiuchi, M. (2011). Identification of chemoattractive factors involved in the migration of bone marrow-derived mesenchymal stem cells to brain lesions caused by prions. *J Virol*, **85**, 11069-11078.

Song, C. H., Honmou, O., Ohsawa, N., Nakamura, K., Hamada, H., Furuoka, H., Hasebe, R. & Horiuchi, M. (2009). Effect of transplantation of bone marrow-derived mesenchymal stem cells on mice infected with prions. *J Virol*, **83**, 5918-5927.

Stahl, N., Borchelt, D. R., Hsiao, K. & Prusiner, S. B. (1987). Scrapie prion protein contains a phosphatidylinositol glycolipid. *Cell*, **51**, 229-240.

Tanaka, M., Fujiwara, A., Suzuki, A., Yamasaki, T., Hasebe, R., Masujin, K. & Horiuchi, M. (2016). Comparison of abnormal isoform of prion protein in prion-infected cell lines and primary-cultured neurons by PrP^{Sc}-specific immunostaining. *J Gen Virol*, **97**, 2030-2042.

Taraboulos, A., Raeber, A. J., Borchelt, D. R., Serban, D. & Prusiner, S. B. (1992). Synthesis and trafficking of prion proteins in cultured cells. *Mol Biol Cell*, **3**, 851-863.

Tobler, I., Gaus, S. E., Deboer, T., Achermann, P., Fischer, M., Rulicke, T., Moser, M., Oesch, B., McBride, P. A. & Manson, J. C. (1996). Altered circadian activity rhythms and sleep in mice devoid of prion protein. *Nature*, **380**, 639-642.

Toyama, K., Honmou, O., Harada, K., Suzuki, J., Houkin, K., Hamada, H. & Kocsis, J. D. (2009). Therapeutic benefits of angiogenetic gene-modified human mesenchymal stem cells after cerebral ischemia. *Exp Neurol*, **216**, 47-55.

Tzaban, S., Friedlander, G., Schonberger, O., Horonchik, L., Yedidia, Y., Shaked, G., Gabizon, R. & Taraboulos, A. (2002). Protease-sensitive scrapie prion protein in aggregates of heterogeneous sizes. *Biochemistry*, **41**, 12868-12875.

Urdzikova, L., Jendelova, P., Glogarova, K., Burian, M., Hajek, M. & Sykova, E. (2006). Transplantation of bone marrow stem cells as well as mobilization by granulocyte-colony stimulating factor promotes recovery after spinal cord injury in rats. *J Neurotrauma,* **23**, 1379-1391.

Uryu, M., Karino, A., Kamihara, Y. & Horiuchi, M. (2007). Characterization of prion susceptibility in Neuro2a mouse neuroblastoma cell subclones. *Microbiol Immunol,* **51**, 661-669.

Veith, N. M., Plattner, H., Stuermer, C. A., Schulz-Schaeffer, W. J. & Burkle, A. (2009). Immunolocalisation of PrP^{Sc} in scrapie-infected N2a mouse neuroblastoma cells by light and electron microscopy. *Eur J Cell Biol*, **88**, 45-63.

Vercelli, A., Mereuta, O. M., Garbossa, D., Muraca, G., Mareschi, K., Rustichelli, D., Ferrero, I., Mazzini, L., Madon, E. & Fagioli, F. (2008). Human mesenchymal stem cell transplantation extends survival, improves motor performance and decreases neuroinflammation in mouse model of amyotrophic lateral sclerosis. *Neurobiol Dis,* **31**, 395-405.

Wadsworth, J. D., Joiner, S., Hill, A. F., Campbell, T. A., Desbruslais, M., Luthert, P. J. & Collinge, J. (2001). Tissue distribution of protease resistant prion protein in variant Creutzfeldt-Jakob disease using a highly sensitive immunoblotting assay. *Lancet*, **358**, 171-180.

Wang, F., Wang, X., Yuan, C. G. & Ma, J. (2010). Generating a prion with bacterially expressed recombinant prion protein. *Science,* **327**, 1132-1135.

Williams, A., Lucassen, P. J., Ritchie, D. & Bruce, M. (1997). PrP deposition, microglial activation, and neuronal apoptosis in murine scrapie. *Exp Neurol*, **144**, 433-438.

Williams, A. E., Lawson, L. J., Perry, V. H. & Fraser, H. (1994). Characterization of the microglial response in murine scrapie. *Neuropathol Appl Neurobiol*, **20**, 47-55.

White, M. D., Farmer, M., Mirabile, I., Brandner, S., Collinge, J. & Mallucci, G. R. (2008). Single treatment with RNAi against prion protein rescues early neuronal dysfunction and prolongs survival in mice with prion disease. *Proc Nati Acad Sci USA*, **105**, 10238-10243.

Wopfner, F., Weidenhofer, G., Schneider, R., von Brunn, A., Gilch, S., Schwarz, T. F., Werner, T. & Schatzl, H. M. (1999). Analysis of 27 mammalian and 9 avian PrPs reveals high conservation of flexible regions of the prion protein. *J Mol Biol*, **289**, 1163-1178.

Yamasaki, T., Baron, G. S., Suzuki, A., Hasebe, R. & Horiuchi, M. (2014a). Characterization of intracellular dynamics of inoculated PrP-res and newly generated PrP(Sc) during early stage prion infection in Neuro2a cells. *Virology*, **450-451**, 324-335.

Yamasaki, T., Suzuki, A., Hasebe, R. & Horiuchi, M. (2014b). Comparison of the anti-prion mechanism of four different anti-prion compounds, anti-PrP monoclonal antibody 44B1, pentosan polysulfate, chlorpromazine, and U18666A, in prion-infected mouse neuroblastoma cells. *PLoS One*, **9**, e106516.

Yamasaki, T., Suzuki, A., Shimizu, T., Watarai, M., Hasebe, R. & Horiuchi, M. (2012). Characterization of intracellular localization of PrP(Sc) in prion-infected cells using a mAb that recognizes the region consisting of aa 119-127 of mouse PrP. *J Gen Virol*, **93**, 668-680.

Yang, Z. X., Han, Z. B., Ji, Y. R., Wang, Y. W., Liang, L., Chi, Y., Yang, S. G., Li, L. N.,

Luo, W. F., Li, J. P., Chen, D. D., Du, W. J., Cao, X. C., Zhuo, G. S., Wang, T. & Han, Z. C. (2013). CD106 identifies a subpopulation of mesenchymal stem cells with unique immunomodulatory properties. *PloS One*, **8**, e59354.

Yoon, S. H., Shim, Y. S., Park, Y. H., Chung, J. K., Nam, J. H., Kim, M. O., Park, H. C., Park, S. R., Min, B. H., Kim, E. Y., Choi, B. H., Park, H. & Ha, Y. (2007). Complete spinal cord injury treatment using autologous bone marrow cell transplantation and bone marrow stimulation with granulocyte macrophage-colony stimulating factor: Phase I/II clinical trial. *Stem Cells*, **25**, 2066-2073.

Zanata, S. M., Lopes, M. H., Mercadante, A. F., Hajj, G. N., Chiarini, L. B., Nomizo, R., Freitas, A. R., Cabral, A. L., Lee, K. S., Juliano, M. A., de Oliveira, E., Jachieri, S. G., Burlingame, A., Huang, L., Linden, R., Brentani, R. R. & Martins, V. R. (2002). Stress-inducible protein 1 is a cell surface ligand for cellular prion that triggers neuroprotection. *EMBO J*, **21**, 3307-3316.

Zhang, Y. K., Liu, J. T., Peng, Z. W., Fan, H., Yao, A. H., Cheng, P., Liu, L., Ju, G. & Kuang, F. (2013). Different TLR4 expression and microglia/macrophage activation induced by hemorrhage in the rat spinal cord after compressive injury. *J Neuroinflamm*, **10**, 112.

Zhou, C., Zhang, C., Zhao, R., Chi, S., Ge, P. & Zhang, C. (2013). Human marrow stromal cells reduce microglial activation to protect motor neurons in a transgenic mouse model of amyotrophic lateral sclerosis. *J Neuroinflamm*, **10**, 52.

Zhu, C., Herrmann, U. S., Falsig, J., Abakumova, I., Nuvolone, M., Schwarz, P., Frauenknecht, K., Rushing, E. J. & Aguzzi, A. (2016). A neuroprotective role for microglia in prion diseases. *J Exp Med*, **213**, 1047-1059.

Zhu, H., Guo, Z. K., Jiang, X. X., Li, H., Wang, X. Y., Yao, H. Y., Zhang, Y. & Mao, N. (2010). A protocol for isolation and culture of mesenchymal stem cells from mouse compact bone. *Nat Protoc*, **5**, 550-560.